

# Experimental investigations of multiple heat storage units utilizing supercooling of sodium acetate trihydrate

## Stability in application size units

**Dannemand, Mark; Englmair, Gerald; Kong, Weiqiang; Furbo, Simon**

*Published in:*
Journal of Energy Storage

*Link to article, DOI:*
10.1016/j.est.2024.111194

*Publication date:*
2024

*Document Version*
Publisher's PDF, also known as Version of record

Journal of Energy Storage 86 (2024) 111194

Contents lists available at ScienceDirect

Journal of Energy Storage

journal homepage: www.elsevier.com/locate/est

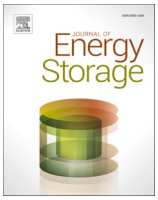

Research papers

# Experimental investigations of multiple heat storage units utilizing supercooling of sodium acetate trihydrate: Stability in application size units

Mark Dannemand *, Gerald Englmair, Weiqiang Kong, Simon Furbo

*Department of Civil and Mechanical Engineering, Technical University of Denmark, Koppels Allé 404, 2800 Kgs. Lyngby, Denmark*

ARTICLE INFO

*Keywords:*
Sodium acetate trihydrate
Supercooling
Phase change material
Heat storage
Stability testing
Spontaneous crystallization

ABSTRACT

Stable supercooling of sodium acetate trihydrate (SAT) composites can be used to store heat over long periods. When the melted SAT is supercooled and in temperature equilibrium with the ambient, the latent heat of fusion is essentially stored without further heat loss. The main limitation of this technology is that the supercooled SAT may crystalize spontaneously and release the stored heat before desired if the storage design does not allow for the principle to work. These investigations elucidate the effects of charge and discharge temperatures and durations on the stability of the supercooling in storage units designed for domestic hot water application.

A test rig with 10 identical heat storage units with water and 35 kg sodium acetate trihydrate composite was set up. Multiple heating and cooling cycles were carried out with charge temperatures between 84 °C and 94 °C for various durations and with discharge temperatures from 10 °C to 35 °C.

The investigations showed that charging the storage units with an inlet temperature of 89 or 92 °C resulted in the highest occurrences of stable supercooling. Discharging with inlet temperatures of 10 °C resulted in higher occurrence of spontaneous solidification during discharge compared to higher inlet temperatures. There was a large deviation in how each tank performed. The best performing tank achieved stable supercooling in 87 % of the test cycles and the worst performing tank achieved stable supercooling in 30 % of the test cycles.

## 1. Introduction

In Europe, the energy consumption in buildings accounts for 40 % of the total energy consumption [1]. Shifting heat demands is pivotal to match with energy supply from renewable energy sources like sun [2] and wind [3]. In this context, thermal energy storage was identified as one key component in future energy systems to utilize renewable energy resources to greater extent [4].

Solar heating systems allow for heating buildings and domestic hot water when solar irradiance is available, and water storage tanks allow for storing heat to the periods immediately following a sunny period [5]. To cover building energy consumption with solar fractions higher than 50 % in central and northern Europe, long-term heat storage is necessary. Additionally, by power-to-heat conversion of excess electricity from sun and wind, buildings-integrated energy stores could serve as one possible source of demand flexibility in future electrical grids [6]. The continuous heat loss from water tanks limits the heat storage period as measured [7] and simulated [8] for solar active houses, utilizing large solar collector arrays for heating.

Alternative heat storage concepts for longer storage periods could be based on phase change materials (PCM) or thermochemical processes [9]. Among other solutions, systems utilizing solid sorption with salt/zeolite composite as investigated by Zettl et al. [10,11], Nonnen et al. [12] and Köll et al. [13], liquid sorption [14] or stable supercooling of PCM [15] may prove useful to integrate more renewable energy for building energy supply and consequently reduce the use of fossil fuels.

### 1.1. Heat storage utilizing stable supercooling of phase change materials

The main advantage of PCMs are high energy storage densities over small temperature intervals across the melting temperature of the PCM [16]. Thus, PCMs are potentially attractive for heat and cold storage [17]. Supercooling is when a melted material cools below the melting temperature without resolidifying, hence remaining liquid. This phenomenon is undesired for short term heat storage because the energy absorbed in the melting process is not released again during discharge. However, the principle can be utilized for long term storage if the melted material remains stable supercooled (without solidifying) in melted

*Abbreviations:* SAT, Sodium Acetate Trihydrate; PCM, Phase Change Material; T, Tank; S, Sensor; U, Upper; M, Middle; L, Lower.

* Corresponding author.
*E-mail address:* markd@dtu.dk (M. Dannemand).

https://doi.org/10.1016/j.est.2024.111194
Received 8 May 2023; Received in revised form 22 November 2023; Accepted 28 February 2024
Available online 8 March 2024

state for the desired duration. When the energy is needed, solidification can be triggered, and the stored heat can be discharged from the material and utilized. A concept for combined short and long-term thermal energy storage can be to utilize the sensible heat of the melted PCM for demands only requiring a short storage period, and the latent heat of fusion in the supercooled PCM for demands requiring long storage periods [18].

Typically, salt hydrates, utilizing stable supercooling, have been considered for long-term heat storage [19], because of large melting enthalpies [20] and low costs as identified by Hasnain [21] and by Garg and Nasim [22]. Xu et al. investigated the thermal behavior of SAT with T-history and full scale tests [23] and Beaupere et al. made experimental measurements on supercooled SAT [24]. Recently, also polyols (polyhydric alcohols) have been investigated as phase change materials for thermal energy storage. They are attractive for their low price, availability in large amounts, high phase change enthalpies (100–413 kJ/kg) and large volume-specific storage capacities [25]. Certain polyols have been identified to have stable supercooling properties. For example, Xylitol could be used with an energy storage capacity of ~580 kJ/l (20–100 °C) – Mixed with 5 % water it has a melting temperature of 91 °C [26]. However, crystal growth rates were reported to be low (below 10 mm/h). Thus, for heat storage application complex nucleation methods would be needed for this material [27]. Puuponnen and Seppälä [28] developed PCM-polymer mixtures containing erythritol or D-mannitol, which showed good long-term performance, stability at low temperatures and higher crystal growth rates in comparison to xylitol-water mixtures.

The first commercial applications of supercooled heat storage, such as hand-warmers, have been realized with the salt hydrate sodium acetate trihydrate (SAT). SAT is non-toxic, available as food supplement, and has a relatively high melting enthalpy (330 kJ/l [29]) at a melting point of 58 °C, which makes it suitable for building energy storage. When SAT supercools below its melting temperature, undissolved sodium acetate separates from the dissolved salt [30], which will reduce the latent heat of fusion in a SAT sample over repeated cycles. Cyclic stable SAT composites with supercooling were achieved by adding thickening agent, water and graphite [31]. The composites showed increased thermal conductivity in solid state but also lower viscosity in melted state. By adding liquid polymeric solutions and water to SAT, cyclic stable SAT composites with higher viscosity in melted state are resulting [32].

Except for long-term heat storage, supercooling is considered as an unwanted effect in PCM applications. To reduce or avoid supercooling of SAT, nucleating agents have been applied in combination with thickening agents as reported by Khan et al. [33] and Wang et al. [34]. Cui et al. [35] proposed nano-copper to form SAT composites with increased thermal conductivity. Without thickening agents, Guion and Teisseire [36] reported sodium-hydrogenophosphte hydrates as nucleating agent for SAT.

### 1.2. Development of long-term heat stores using sodium acetate trihydrate

Flat [37] and cylindrical [38] prototype heat storage units have been tested at the Technical University of Denmark. Four flat storage units each containing approx. 150 l SAT composite was tested in combination with a water tank [39]. This setup was used in a solar heating and hot water supply system with evacuated tubular collectors [41]. Experimental results were used to verify a numerical simulation model, which was then used to study the system performance in a Danish Passive House [42]. Results show that heat stores utilizing stable supercooling of SAT composites could be charged several times during winter with surplus energy from wind and in summer, spring and autumn by solar collectors.

The major challenge in application scale is the stability of the supercooling. Unwanted, spontaneous solidification occurs due to formation of crystal nuclei in the supercooled liquid. Mullin [45] defined two kinds of nucleation: From solution (when a nuclei is formed within the supercooled liquid) or due to the presence of existing crystals (introduced to the supercooled liquid).

In heat storage using supercooling of SAT, nucleation from solution may occur due to impurities acting as nucleation agents in the SAT mixture. Also, SAT composites will recrystallize when they cool down if not all parts of the storage are heated to sufficiently high temperatures to ensure full dissolving of sodium acetate in water [46]. Nucleation due to presence of existing crystals must be avoided by means of appropriate heat storage design. Unsmooth surfaces or cracks in the metal container or heat exchangers may cause nucleation in a similar way as flexing the metal disc in hand warmers [47]. Furthermore, containers must be closed in order to avoid introduction of seed crystals via the air. The roughness of the container surface may have an effect on the supercooling as investigated by Awasthi et al. [48].

On-demand crystallization of supercooled SAT composites can be either initialized by introducing a seed crystal e.g. by injection or crystallization can be initiated by rapid local cooling to temperatures below −15 °C utilizing Peltier elements or CO2 evaporation [44]. Crystallization velocities has been reported by Dietz et al. [43] and the nucleation in heat packs has been investigated by Rogerson and Cardoso [29].

Wang et al. [49] and Shamseddine et al. [51] have made comprehensive reviews of SAT with supercooling as a heat storage material.

Several authors have applied SAT in various systems and reported their findings. Kutlu et al. have coupled a SAT heat storage with a heat pump system [52]. Wang et al. have applied industrial grade SAT in a plate heat storage unit [53]. Chen has investigated the heat transfer of a shell and tube heat storage tank with SAT [54]. Zhou et al. have applied SAT in space heating systems [55].

### 1.3. Investigations on supercooling stability

During application, heat is stored and released in repeated melting, supercooling and solidification processes, referred to as test cycles in this work. Applied methodology for thermal cycling tests of materials was reviewed by Ferrer et al. [56], concluding need for a common standard. One example are test regulations by the German “RAL Gütegemeinschaft PCM e.V.”, as applied for material development by Rathgeber et al. [57].

In previous work at DTU [58], a heat loss method has been applied to identify promising SAT composites with stable supercooling properties. Samples with a variety of additive concentrations were tested. Later, Dannemand et al. [37,38], Englmair et al. [32,39] and Wang et al. [40,50] have investigated prototype storage units with heat exchangers, designed to enable stable supercooling with identified promising SAT composites. The investigations were focusing on the heat transfer and the applicability of stores for domestic applications. In their investigations, the supercooled SAT solidified spontaneously in some of the tests. They did, however, achieve stable supercooling up to several months in some tests. As reported by Rathgeber et al. it is important to test PCM material under application conditions as the PCM may act differently compared to small scale material investigations [59].

### 1.4. Aim and scope

In order to assess the long-term performance of a PCM in storage unit, stability tests under repeated thermal cycling are crucial [60]. The key for having a reliable storage utilizing supercooling of SAT composites is to have a design of the storage tanks and heat exchangers where the SAT can remain stable supercooled in the desired storage period. The main aim of these investigations has been to elucidate how a SAT composite performed related stability of supercooling in a tank design made for application in buildings’ heating systems. Previous studies [30,31,58] have shown that SAT composites supercool stable in a reliable way in sample sizes of around 200 g in glass jars, but not always in metal tanks with up to 200 kg PCM [15,32,37,38]. It is essential to

determine how reliable the stable supercooling is in units designed for application; if there is a systematic behavior of spontaneous crystallization which can be addressed or if spontaneous solidification occurs randomly. Therefore, it is essential to investigate over many repeated cycles, whether there in a specific storage design occurs spontaneous solidification, and if individual storage units with similar design perform differently.

This work aims to elucidate barriers in moving the technology closer to real application by investigating the cycling stability, including supercooling, in multiple tanks with a design which is ready for application and can be mass produced. The stability of the supercooling of SAT composites in ten identical domestic hot water tanks with PCM in mantles of the tanks [61], have been investigated. The focus of this study was to investigate under which charge and discharge conditions the SAT composite remained supercooled. For this purpose, different charging temperatures and periods, and discharging temperatures were applied.

Further, the investigations aimed to elucidate if the spontaneous solidification started during the discharge or from the supercooled standby period and if it started from specific locations in the storage unit or from random locations.

The authors have not found research in the literature, which to this extent have investigated the stability of supercooling of SAT composites in storage tanks over repeated tests and elucidated the effect of charge and discharge temperatures. The authors believe that the work presented in this article will provide valuable knowledge for future development of heat storage with supercooled SAT.

## 2. Method and experimental setup

A test rig with 10 identical heat storage units with water and PCM was installed in a laboratory at the Technical University of Denmark. Multiple heating and cooling test cycles with various charge and discharge temperatures and durations were carried out with the tanks. This was done to develop data for evaluating the stability of the supercooling of SAT in the heat storage tanks from an industrial production line and to elucidate the effects of the charge and discharge conditions.

### 2.1. The heat storage units

The heat storage units were developed by H.M. Heizkörper GmbH & Co. KG under the product name “LOT – Latent On Top”. The tank was a 150 l hot water storage tank with internal heat exchanger spirals for a solar collector loop and an auxiliary heating source. The heat exchanger spirals were not used in these investigations. The cold-water inlet was located in the bottom of the tank. The hot water outlet was made with a pipe extracting water from the top of the tank, down through the tank and exiting at the bottom of tank. This was to avoid thermal bridges in the upper part of the storage. The height of the tank was 1.65 m. The inner diameter of the water tank was 356 mm. A 1.4 m high mantle was welded to the outside of the water tank so that it enclosed the majority of the water tank on the sides, See Fig. 1. The thickness of the mantle chamber was 20 mm. The tank was insulated with 90 mm PUR-foam.

The mantle was only partly filled and contained 35 kg of SAT composite. The composite was developed by the manufacturer of the storage unit and patented in Europe with the number EP 3438225 A1. The latent heat of fusion of the SAT composite at 58 °C has been determined to 240–264 kJ/kg [41]. The density and specific heat capacities have not been measured for this specific SAT composite. Heat was transferred between the water and the PCM through the tank wall. The tanks were constructed with standard stainless steel plates. No measures were taken to reduce roughness of surfaces of the PCM chamber. The mantle containing the PCM was open to the ambient via an air filter on a pipe connected to the top part of the PCM mantle. This semi-open design of the PCM chamber was made to avoid pressure changes in the PCM mantle during expansion and contraction of the SAT while minimizing particles in the ambient air entering the PCM chamber and potentially triggering the solidification undesired.

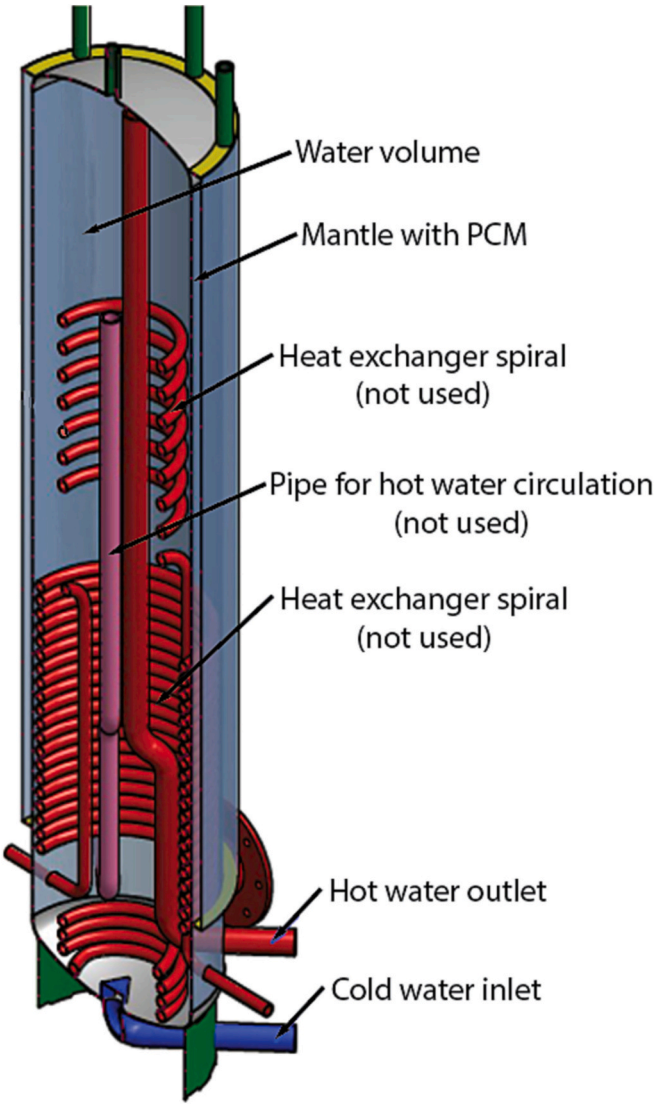


**Fig. 1.** Storage tank diagram with heat exchangers, in- and outlet and mantle with PCM. (Reference: H.M. Heizkörper).

To trigger the solidification of the supercooled SAT actively, SAT crystals were blown into the top of the PCM mantle with an air compressor when needed. This device is referred to as the crystal blower. Crystal blowers were mounted on top of each tank.

### 2.2. The 10 unit hydraulic loop

Ten identical tanks, shown in Fig. 2, were connected to a pipe loop allowing for charging and discharging the tanks in parallel. A test rig for heating and cooling allowed for controlling the temperatures during charge and discharge of the tanks. Each tank was heated and cooled via direct inlet of water into the bottom part of the tank through the cold-water inlet. The outlet from each tank was from the top of the tank through the hot water outlet. For both charge and discharge the flow direction was into the bottom of the tank and out from the top. A schematic of the test rig with the ten storage units is shown in Fig. 3.

A pump circulated the water in the loop and through the tanks. Regulation valves and flow meters at the inlets of each tank were used to adjust the flow through the tanks to be the same for all tanks. The flow rate through each tank was approximately 150 l per hour.

During charging, the water in the loop was heated with electric

**Fig. 2.** Test rig installation with the 10 identical heat storage units.

heating elements with a power of 27 kW. A PID controller, integrated in the test rig, was used to set the maximum forward temperature of the water in the loop to a set temperature. During discharge, heat was discharged via a heat exchanger to a central cooling system in the laboratory. A thermostatic valve with temperature sensitive sensor was used to discharge the tanks down to the desired temperature level. This mechanical valve with limited accuracy allowed for discharging to a temperature with up to ±2.5 K deviation of the desired level.

During the experiments, the 150 l of water in each tank was heated during charge and cooled during the discharge. Heat was transferred between the water and the PCM in the mantle through the tank wall.

### 2.3. Measurements, data logging and the automated control

DS18B20 digital temperature sensors with an accuracy of 0.5 K were used to measure the temperatures of the tank surfaces, the water temperature in the tanks and the forward and return temperatures before and after the cooling and heating element. On each of the ten tanks (T01–T10), 12 digital temperature sensors were placed on the outer surface of the PCM mantle in good thermal contact with the tank wall under the insulation. Four sensors were located in the upper (U) area of the PCM mantle (TxxS1U, TxxS2U, TxxS3U, TxxS4U), four in the middle (M) area (TxxS1M, TxxS2M, TxxS3M, TxxS4M), and four in the lower (L) area of the mantle (TxxS1L, TxxS2L, TxxS3L, TxxS4L). All evenly distributed along the circumference of the PCM mantle. One additional sensor was located in the middle of the water volume (TxxS1W) to measure the water temperature. The location of the temperature sensors on each tank are displayed in Fig. 4. A total of 132 digital temperature sensors were used to monitor the temperatures in the ten tanks. The purpose of having the temperature sensors distributed over the surface of the mantle was to elucidate where the solidification of the started.

A LabVIEW programmed control interface was used to log the temperature measurements and to control the test cycles. The measurements were logged with one minute intervals. An Arduino was used to run the LabVIEW program, which controlled the pump in the pipe loop, the heating elements and the motor valves for controlling the flow of heat transfer fluid in the central cooling system. The air compressors for initiating solidification were also controlled by the LabVIEW program. An integrated function was used to detect a sudden temperature increase and logged the order of the sensors where a temperature increase occurred for each tank. This showed which sensor recorded a temperature increase first after the solidification of the supercooled PCM and gave an indication of where the solidification started.

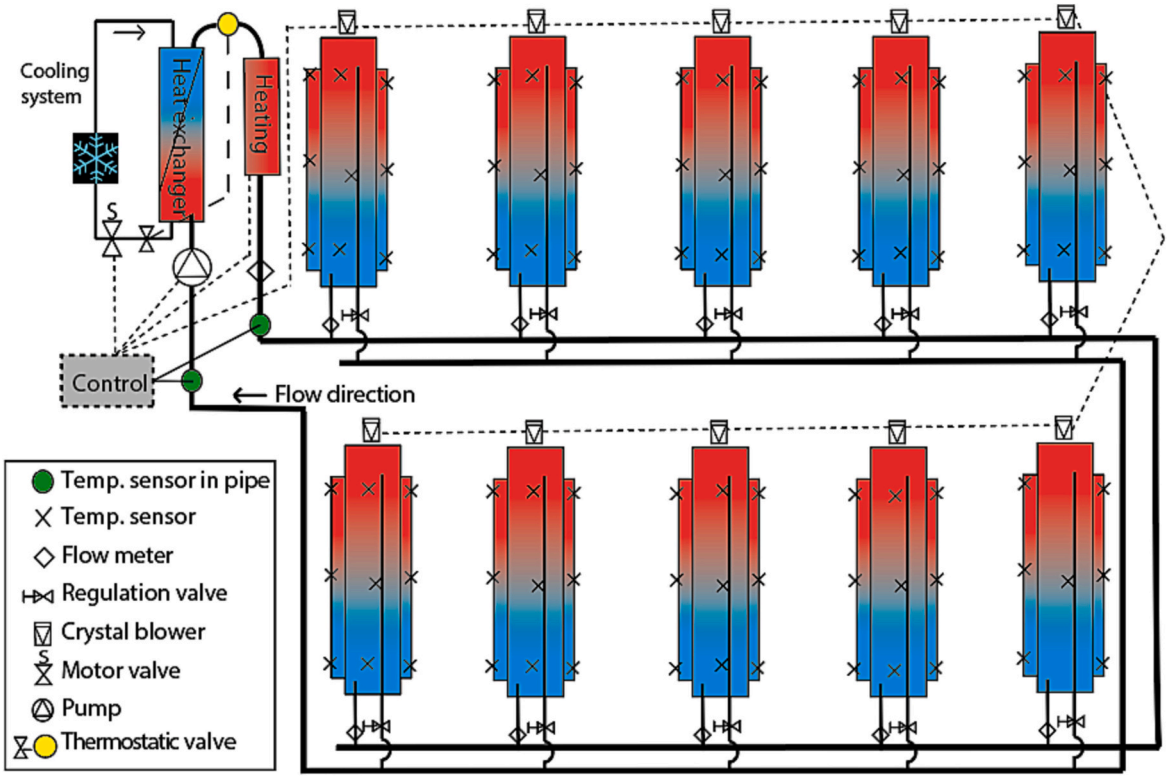


**Fig. 3.** Diagram of pipe loops incl. Heating and cooling system, temperature sensors, valves, pump and the ten storage tanks connected in parallel.

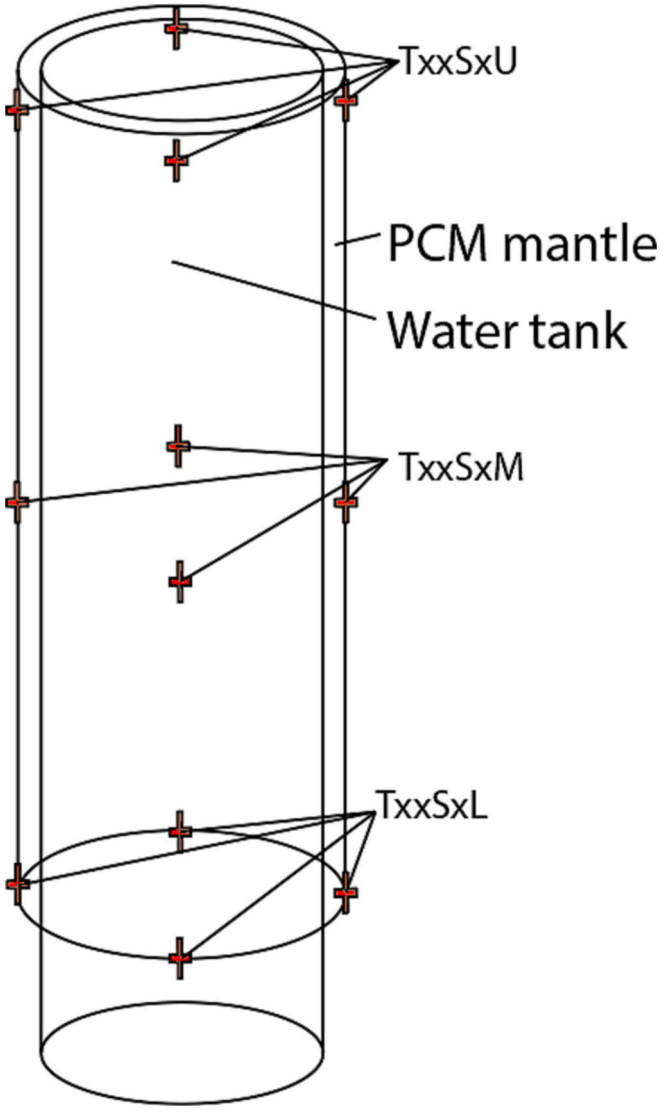


**Fig. 4.** Location of temperature sensors (TxxSxU, TxxSxM, TxxSxL) on the PCM mantle of the storage units.

### 2.4. PCM behavior

In the context of current research where utilizing supercooling of the PCM is desired, the following terminology is used. *Stable supercooling* is defined to be when the PCM remains in melted and supercooled state after being cooled below its melting point and the PCM remains in supercooled state until the solidification is intentionally triggered. *Spontaneous solidification* is defined as when the supercooled PCM solidifies before it is intentionally triggered. This may occur during the discharge phase or from the standby phase when it has been cooled to a desired temperature and the active discharging has stopped.

### 2.5. Experiments

Two different types of test series were carried out. The test cycles in "experiment A" focused on the effect of different discharge temperatures while charging the tanks until minimum temperatures were reached by all temperature sensors on the surface of the PCM mantle. The test cycles in "Experiment B" focused on the effect of different charge duration and different charge temperatures with a fixed discharge temperature simulating a cold-water temperature. Each of the selected test cycle conditions (charge and discharge temperatures and durations) were repeated 5–7 times to form a better statistical basis for the evaluation. The experiments carried out with similar charge and discharge temperatures and durations are referred to as a "test series" in Table 1 and Table 2.

The stability of the supercooling was evaluated based on if spontaneous solidification occurred before the crystal blower triggered the solidification. It was distinguished whether the spontaneous solidification occurred during the discharge period or if it occurred during the supercooled standby period. The supercooled standby period was defined as the period after the discharge flow was stopped and until the crystal blower was activated.

#### 2.5.1. Experiment A: Charge to a set mantle temperature – different discharge temperatures

A test cycle in "Experiment A" consisted of the following states:

1. Charge the tanks with a fixed inlet temperature until a set minimum temperature was reached for all the temperature sensors on the surface of the PCM mantle. Two different temperature levels were investigated. An inlet temperature of 87 °C until all sensors reached 78 °C and an inlet temperature of 92 °C until all sensors reached 83 °C.
2. Standby period in the heated state for 3 h without flow through the tanks.
3. Discharge (sensible heat) until a set temperate for all sensors in the tanks was reached. Different discharge temperature levels were applied ranging from 6 °C to 37 °C.
4. Standby in supercooled state for 3 days with no flow through the tanks.
5. Initialization of crystallization.
6. Standby for 3 h to let the heat transfer from the PCM to the water.
7. Discharge of the reheated water (latent heat from PCM) until a set temperate for all sensors in the tanks was reached.

An additional variation of the test cycles was made with 6 and 12 h standby periods in the heated state instead of 3 h. This was done to elucidate if a longer standby period in the heated state would affect the supercooling. This variation was done for charging with 87 °C until the temperature sensors had reached 78 °C and an outlet temperature of 10–16 °C. A total of 55 cycles were carried out with the 10 units in the experiment A. Table 1 displays an overview of the test cycles carried out in experiment A.

#### 2.5.2. Experiment B: Charge with different temperatures and durations – fixed cold discharge

The "experiment B" test sequence was:

1. Charge with an inlet temperature of 84 °C, 89 °C or 94 °C for 8, 10, 12 or 16 h.
2. Standby in heated state for 1 min.
3. Discharge (sensible heat) for 8 h with an inlet temperature of approximately 10 °C (due to the mechanical valve controlling the discharge temperature the actual inlet temperature varied between 7 and 11 °C.
4. Standby in supercooled state for 3 days.
5. Initialization of crystallization.
6. Standby period of 3 h to let the heat transfer from the PCM to the water.
7. Discharge of reheated water (latent heat from PCM) with an inlet temperature of approximately 10 °C for 8 h.

Table 2 summarizes the conditions for the test cycles and the temperatures for charge and discharge. A total of 69 test cycles were carried out in experiment B.

**Table 1**
Overview of test cycles in experiment A.

| Test series no. | No. of repeated test cycles | Heating element set point [$^0$C] | Surface sensor minimum temperature for end charge [$^0$C] | Standby period in heated state [hours] | Discharge inlet temperature range (average) [$^0$C] | Surface sensor maximum temperature for end discharge [$^0$C] |
|---|---|---|---|---|---|---|
| 1 | 5 | 87 | 78 | 3 | 13–14 (13.4) | 24 |
| 2 | 6 | 87 | 78 | 3 | 20–25 (21.7) | 27 |
| 3 | 7 | 87 | 78 | 3 | 28–30 (29.2) | 32 |
| 4 | 6 | 87 | 78 | 3 | 33–37 (35.6) | 38 |
| 5 | 6 | 92 | 83 | 3 | 6–12 (9.3) | 18 |
| 6 | 6 | 92 | 83 | 3 | 18–25 (23.8) | 25 |
| 7 | 6 | 92 | 83 | 3 | 27–30 (28.4) | 32 |
| 8 | 6 | 87 | 78 | 6 | 10–16 (13) | 20 |
| 9 | 7 | 87 | 78 | 12 | 10–12 (11.4) | 20 |

**Table 2**
Overview of test cycles in experiment B.

| Test series no. | No. of test cycles | Heating element set point [$^0$C] | Duration of heating [hours] | Discharge inlet temperature Range (average) [$^0$C] |
|---|---|---|---|---|
| 10 | 6 | 84 | 8 | 7–9 (7.3) |
| 11 | 7 | 84 | 10 | 8–10 (9.0) |
| 12 | 6 | 84 | 12 | 7–9 (8.0) |
| 13 | 6 | 84 | 16 | 7–10 (8.6) |
| 14 | 6 | 89 | 8 | 8–11 (9.9) |
| 15 | 6 | 89 | 10 | 9–10 (9.5) |
| 16 | 7 | 89 | 12 | 8–10 (8.8) |
| 17 | 7 | 89 | 16 | 8–10 (8.8) |
| 18 | 6 | 94 | 8 | 9–10 (9.8) |
| 19 | 6 | 94 | 10 | 9–11 (9.9) |
| 20 | 6 | 94 | 12 | 8–9 (8.8) |

## 3. Results and discussions

In the following, temperature developments during test cycles are presented. Supercooling stability was evaluated.

### 3.1. Test cycle examples

Measurements from selected test cycles are shown in Fig. 5 to Fig. 11. Details of a test cycle with 3 days stable supercooling, a test cycle with spontaneous solidification during discharge and a test cycle with spontaneous solidification in the standby period are presented.

#### 3.1.1. Stable supercooled

Fig. 5 displays the measured temperatures and the heating and cooling settings for a test cycle with a tank where the SAT remained stable supercooled for 3 days and then triggered by the crystal blower. Typically at the end of the charge process, the sensors TxxS1L had the highest temperature and the sensors TxxS3L had the lowest temperaure.

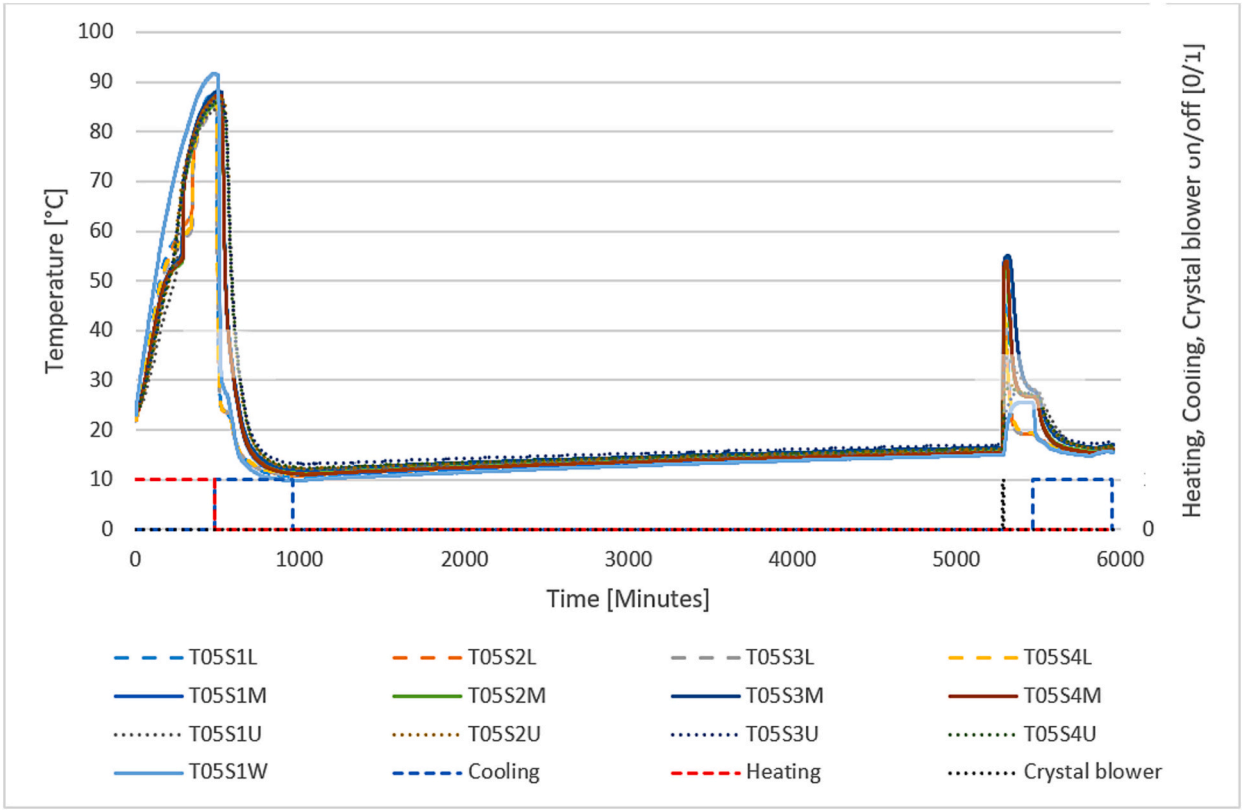


**Fig. 5.** Temperature development in tank 5 during test, experiment B, test cycle 18, where the SAT was supercooled for 3 days before solidification was triggered with the crystal blower. Charge period was 8 h with an inlet temperature of 94 °C.

This temperature distribution may be related the flow rate, the location and the shape of the inlet.

Fig. 6 shows the temperatues at the end of the charge period. At the start of the discharge it can be seen that the temperture in the lower part of the tanks dropped first as expected, when the discharge of hot water was from the top and inlet of cold water to the bottom.

Fig. 7 shows the measured temperature increase of the sensors in the tank after the solidification of the supercooled SAT was triggered by the crystal blower. Triggering occurred without flow through the tank. The temperature increase started at T04S1U in the upper part of the SAT mantle near the crystal blower. The water temperature increased 10–12 K. It can be seen that the temperatures for the M sensors reached 54 °C, close to the melting temperature of SAT. The lower sensors L did not reach the same temperature level most likely because they are located at the very bottom of the PCM mantle and did not receive as much heat from the solidifying SAT because of higher heat transfer away from this area due to the geometry. The temperature of the upper sensors U increased even less and appeared to measure the temperature on the outside of the mantle at the air volume above the PCM.

#### 3.1.2. Spontaneous solidification during discharge

Fig. 8 shows an example of a test cycle where the SAT solidified spontaneously during discharge.

Fig. 9 shows the details of the temperature development for the spontaneous solidification. The temperature in the bottom of the tank dropped first as the discharge was from the top and the cold inlet was into the bottom. The sudden temperature increase from the solidification started at the bottom sensors and was followed by the middle and upper sensors indicating the solidification started from the bottom. The spontaneous solidification occurred in the 580th minute time step during the discharge in this example.

#### 3.1.3. Spontaneous solidification from standby period

Fig. 10 shows an example of a test cycle where spontaneous solidification occurred in the standby period approxinatly 16 h after the end of the first dischage phase.

Fig. 11 shows in detail the temperature development when the spontaneous solidification occurred. In this case, it can be seen that the senor T07S1L at the bottom of the tank started to increase first. This indicates that the solidification started from the bottom of the PCM mantle.

### 3.2. Experiment A: Charge to a set mantle temperature – different discharge temperatures

For the test cycles in experiment A with charging until a specific temperature for all the temperature sensors was reached, the charging duration varied within test cycles with identical test conditions. The charge duration varied between 10 and 14 h for the test cycles with discharge temperatures around 10 °C in test series 1 and between 8 and 9 h for the test cycles with discharge temperatures around 35 °C in test series 4.

On Fig. 12 to Fig. 14 the vertical error bars represent the standard deviations of the occurrence in each test series. The horizontal error bars represent the full temperature range in each of the test series. Trend lines for each temperature interval are included. The discharge temperature on the x axis represents the final temperature the tanks were discharged to.

Fig. 12 shows how often stable supercooling for 3 days occurred for the various charge temperatures and discharge temperatures – it occurred in up to 85 % of the test cycles when the tanks were charged with an inlet temperature of 92 °C and the discharge temperatures was 25-30 °C. The different test series show clearly that charging with an inlet temperature of 92 °C resulted in a higher occurrence on stable supercooling compared to charging with an inlet temperature 87 °C. Further, it also shows that discharging with higher inlet temperatures resulted in more stable supercooling. However, increasing the discharge inlet temperature from 22 °C to 30 °C after being charged with an inlet

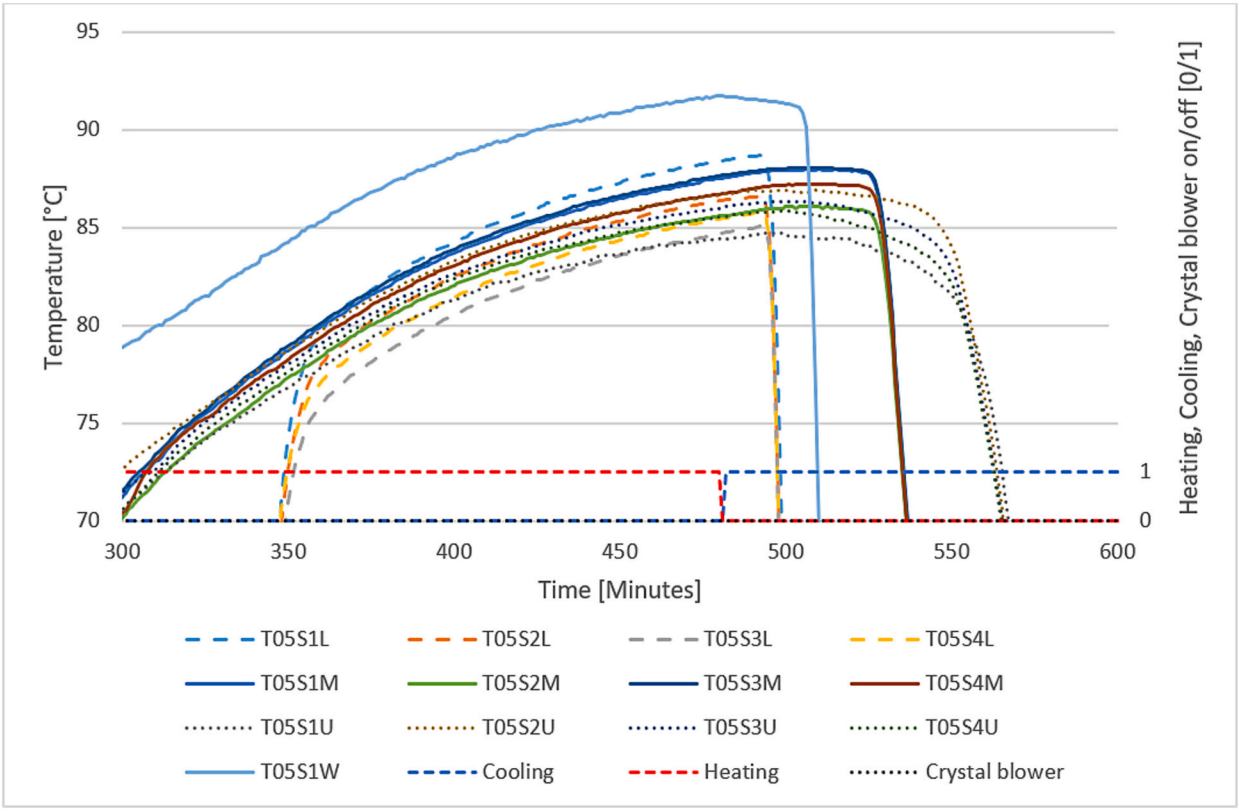


**Fig. 6.** Detail of temperature development at the end of the 8 h charge period and start of the discharge for a test with tank 5 in experiment B, test series 18,.

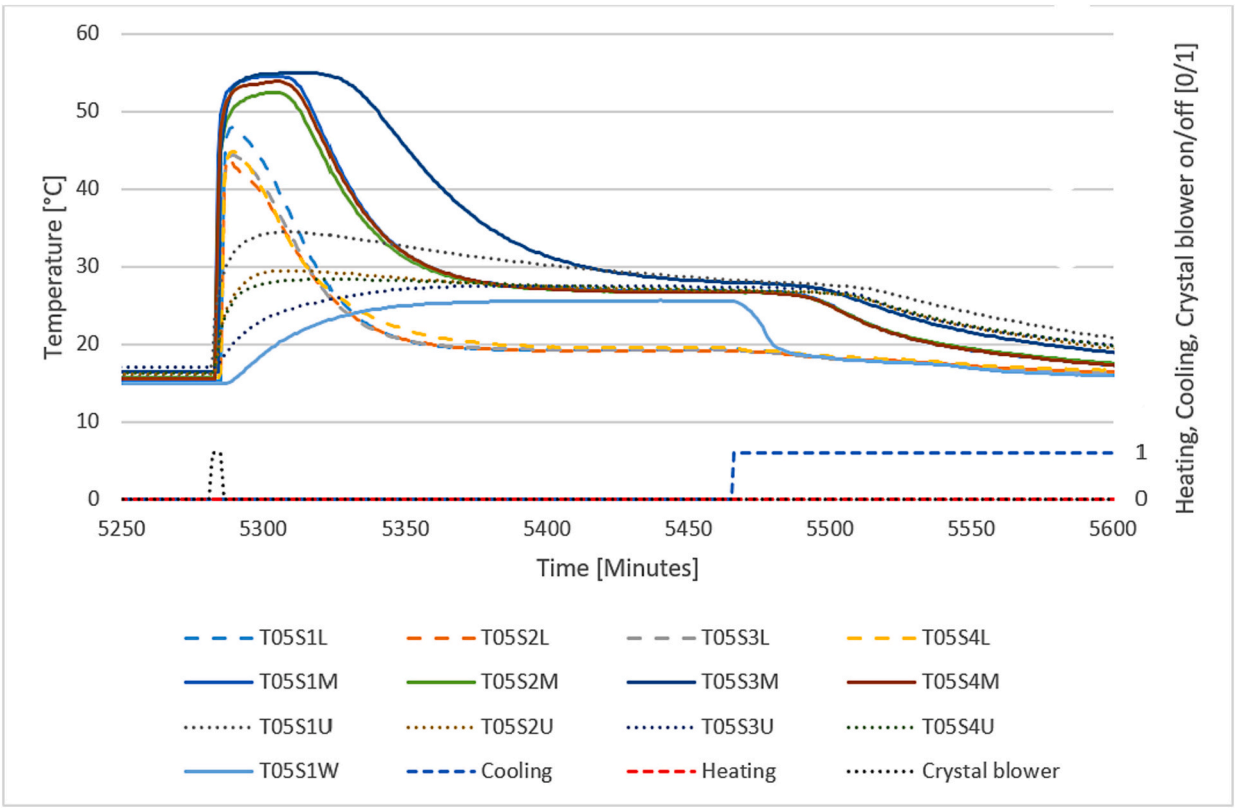


**Fig. 7.** Details of temperature development in tank 5 after the triggered solidification in experiment B, test series 18, showing the temperature increase, the 3 h standby and the following discharge.

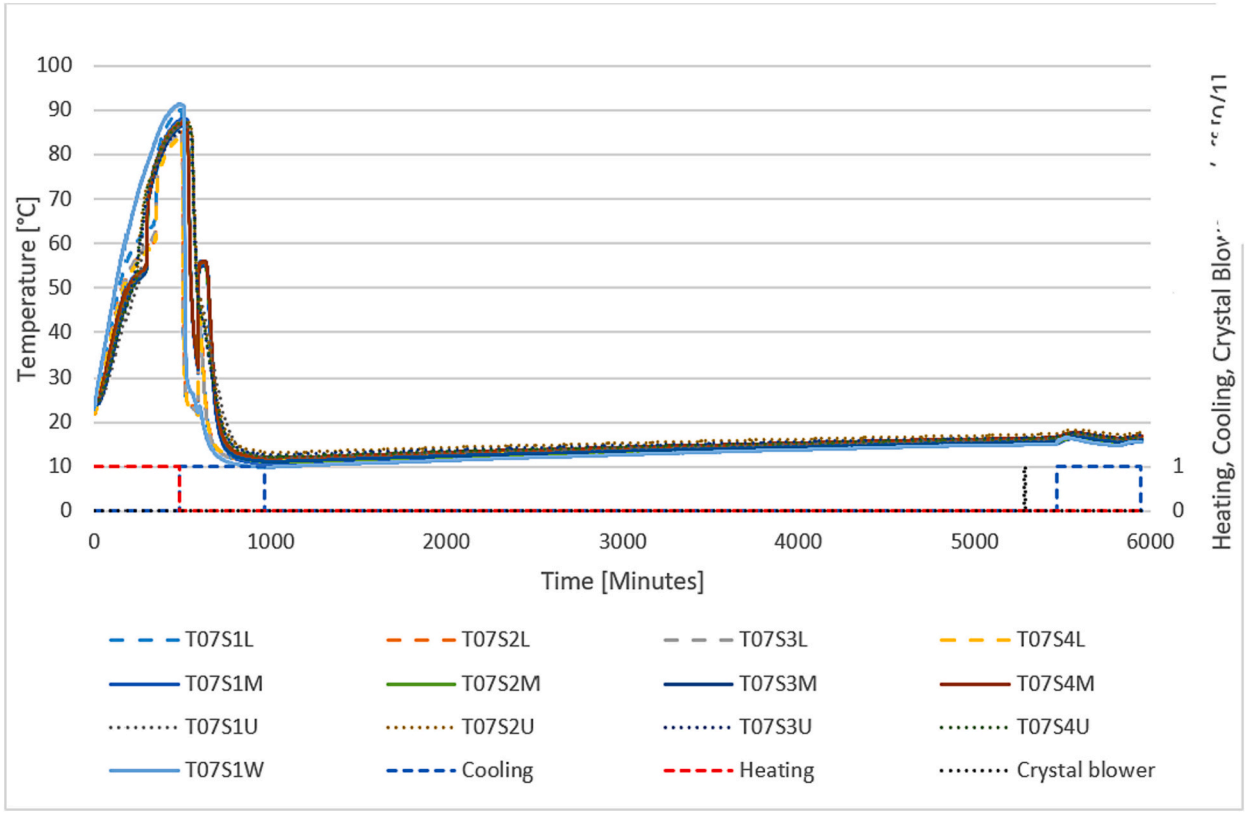


**Fig. 8.** Temperature development in tank 7 during test experiment B, test series 18, where solidification occurred spontaneously during discharge after 8 h charge with an inlet temperature of 94 °C.

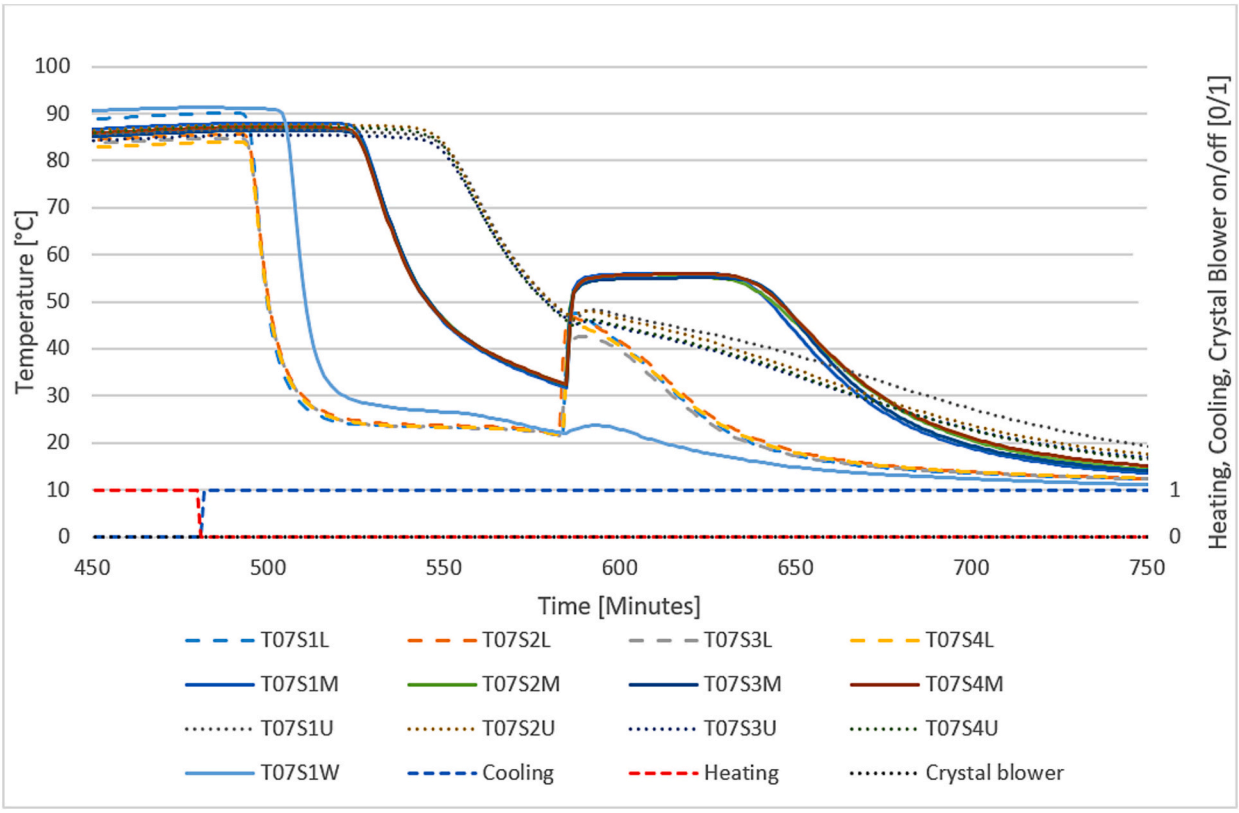


**Fig. 9.** Detail showing the temperature development after spontaneous solidification during first discharge period after being charged for 8 h with an inlet temperature of 94 °C.

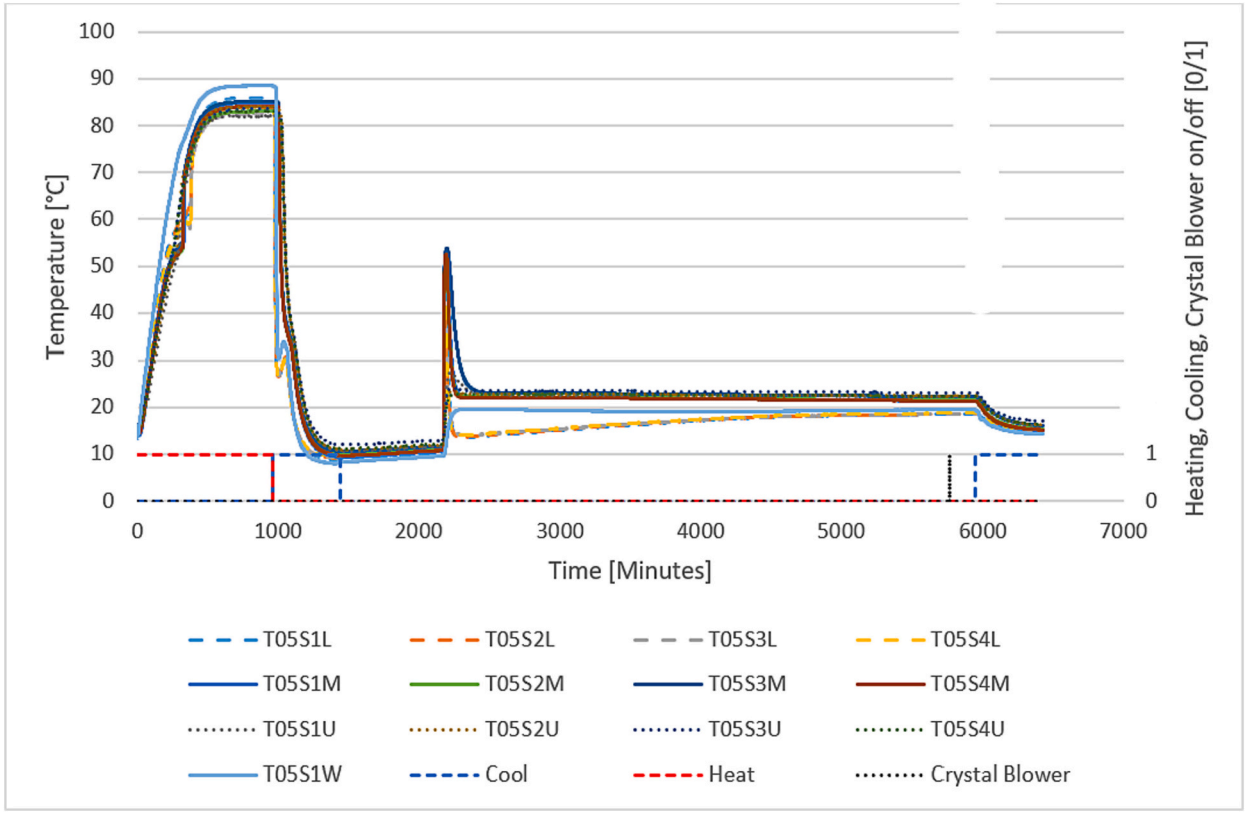


**Fig. 10.** Temperature development in tank 5, experiment B, series 17, where solidification started spontaneously from the standby period after being charged with an inlet temperature of 89 °C for 16 h.

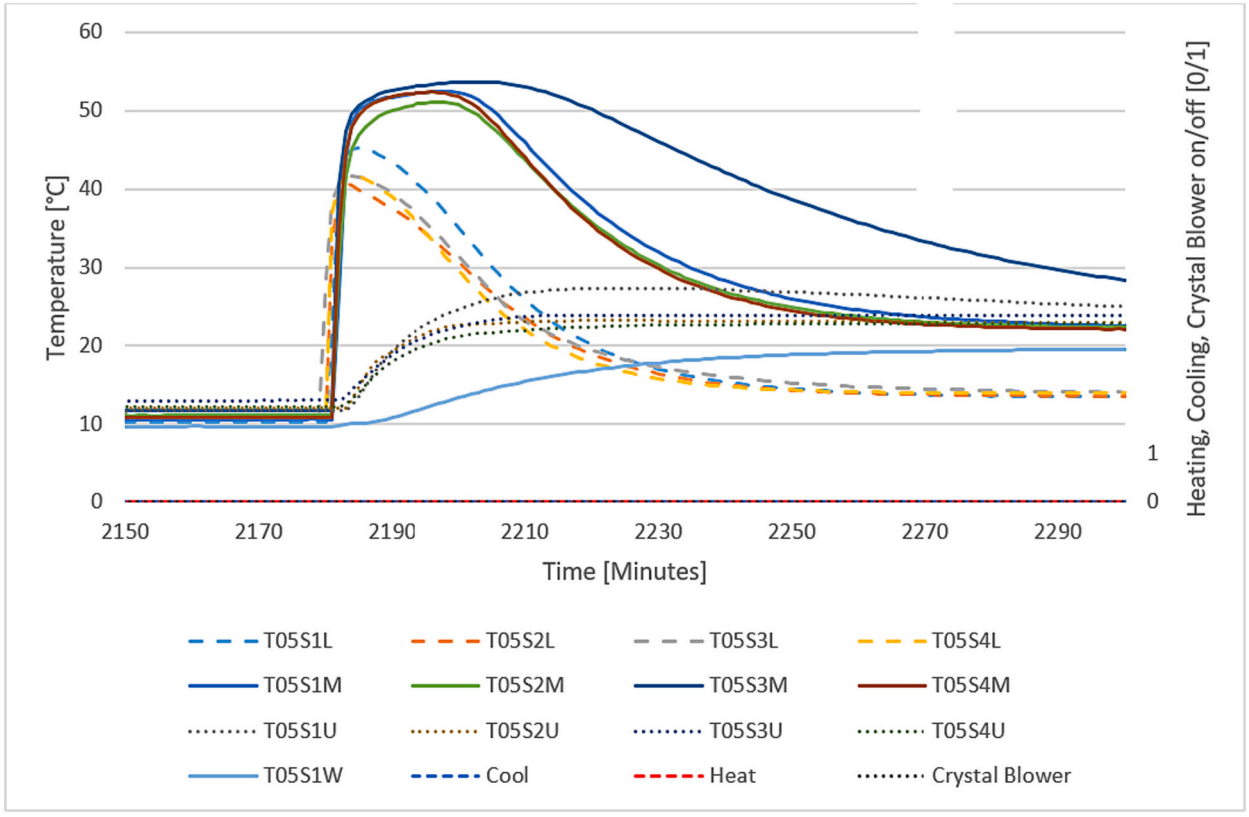


**Fig. 11.** Detail of temperature development in tank 5 after spontaneous solidification started from supercooled standby period.

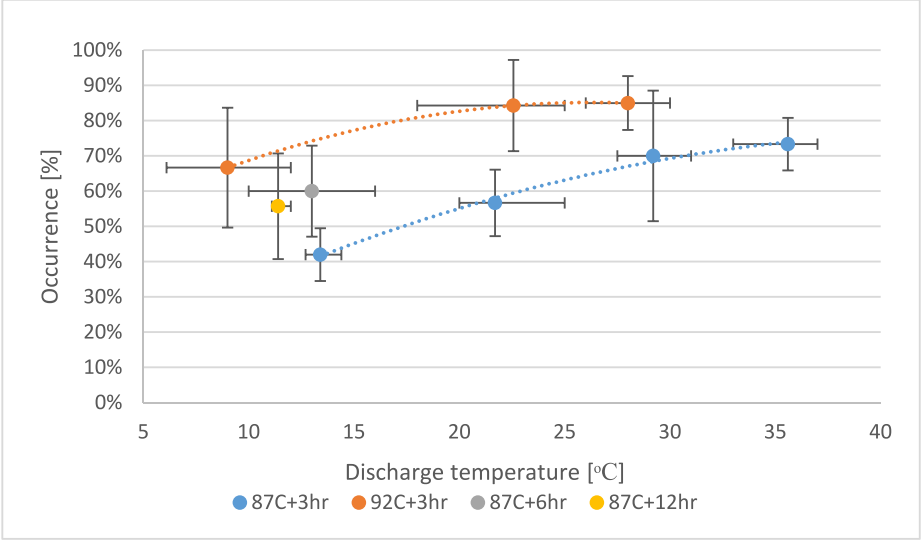


**Fig. 12.** The percentage of test cycles which achieved 3 days stable supercooling in the test cycles in experiment A shown with standard deviation and temperature range.

temperature of 92 °C and increasing the inlet temperature from 29 °C to 35 °C after charging with 87 °C only improved the stability of the supercooling by 1 %.

Comparing test series 1, 8 and 9 with similar charge temperature and durations but different standby periods in the heated state, showed that leaving the tank in heated state for 6 h resulted in a more stable supercooling compared to leaving the tanks in heated state for 3 h. However, 12 h of standby in the heated state resulted in lower stable supercooling compared to 6 h.

Fig. 13 shows that heating the units to 92 °C resulted in fewer cases of spontaneous solidification during discharge compared to heating the units to 87 °C. The difference was more obvious with lower discharge temperatures.

The occurrence of spontaneous solidification during the standby period dropped significantly with higher charge temperature as shown in Fig. 14. In addition, the longer standby period in the heated state resulted in reduced spontaneous solidification.

As the hot water in the tanks was replaced with colder water at the

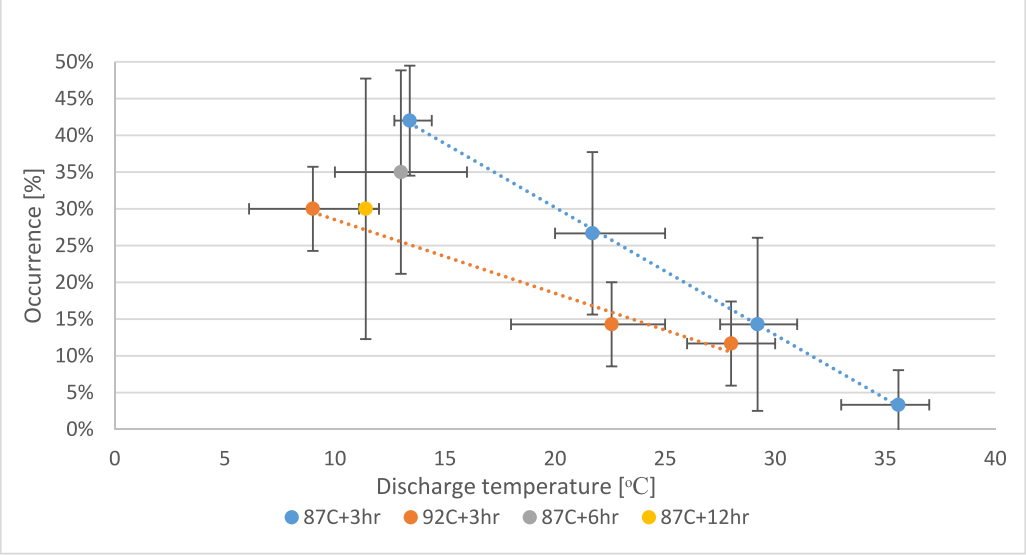


**Fig. 13.** The percentage of tests where spontaneous solidification occurred during discharge for the test cycles in Experiment A.

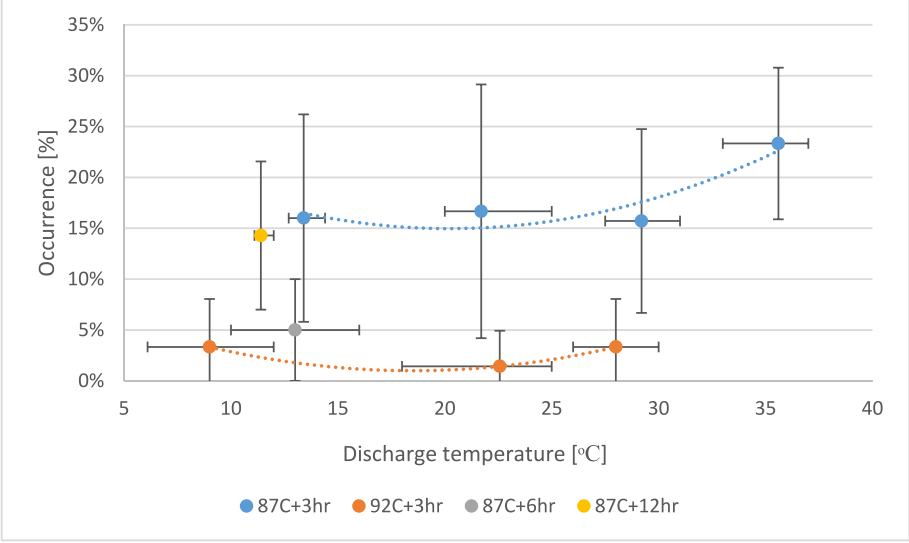


**Fig. 14.** Percentage of tests where spontaneous solidification started from the cold standby period after being charged with 87 °C or 92 °C and discharged with temperatures ranging from 6 °C to 37 °C.

start of the discharge, the discharge power, for each tank, peaked at up to 14 kW after the tank had been charged to 92 °C and discharged to 10 °C. When the tanks had been charged to 87 °C and discharged to 30 °C, the discharge power peaked at 8.5 kW for each tank at the beginning of the discharge.

### *3.3. Experiment B: Charge with different temperatures and durations – fixed cold discharge*

Fig. 15 shows for each test series how often stable supercooling was achieved for the 3-day period. Charging for 10 h with an inlet temperature of 89 °C had the highest occurrence of stability across all the scenarios. Charging for 12 or 16 h at 89 °C resulted in fewer cases of stable supercooling. Charging with 89 °C compared to 84 °C clearly resulted in higher stability. Charging for 12 h resulted in the highest occurrence of stability for charging with 84 °C. Charging for 8 h resulted in the highest occurrence of stability for charging with 94 °C. Charging with 94 °C did not improve the stability compared to charging with 89 °C.

The surface temperatures at the end of the charge period ranged from 2 to 8 K below the water temperature in the tank depending on the location of the sensors.

In Fig. 15 to Fig. 17 the error bars represent the standard deviation. The points are shifted slightly off the values on the x-axis to avoid overlapping of the error bars. Charge periods were 8, 10, 12 or 16 h for all tests. Trend lines for each temperature interval are included. Across all the test cycles, the average discharge temperature was 8.9 °C with a variance of 2.3 K.

Fig. 16 shows that increasing the charge temperature from 84 °C to 89 °C led to fewer cases of spontaneous solidification during the discharge. Charging at 94 °C showed not to reduce the cases of spontaneous solidification further, but increased the occurrence compared to 89 °C.

Fig. 17 shows that for charge temperatures of 89 °C and 94 °C, shorter charge durations resulted in fewer cases of spontaneous solidification in the supercooled standby period. However, for charging with

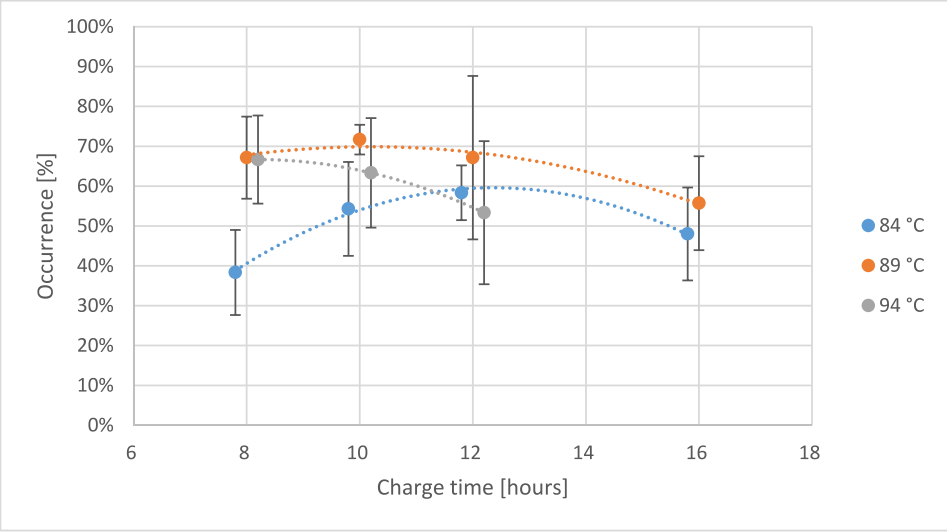


**Fig. 15.** Percentage of supercooling stability in experiment B with various charge temperatures and durations. Discharged to 10 °C.

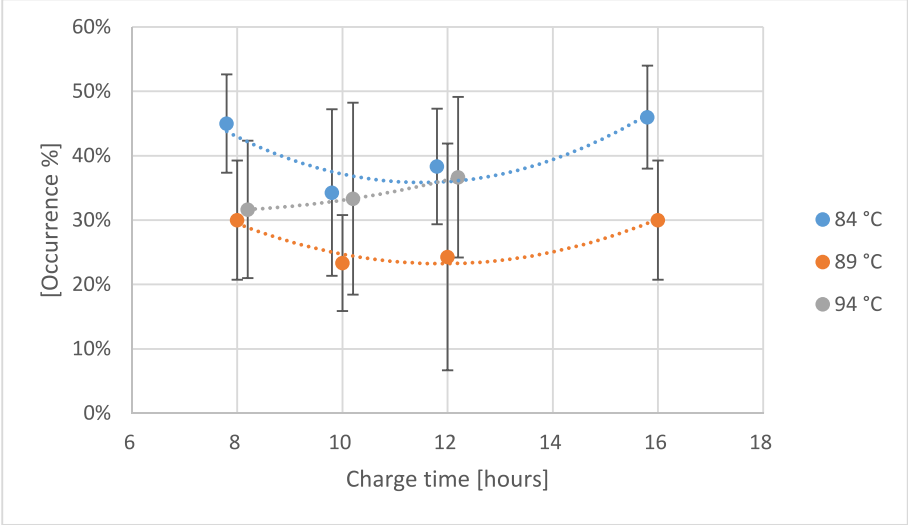


**Fig. 16.** Occurrence of spontaneous solidification during discharge for charge temperatures and durations of 84 °C, 89 °C and 94 °C for 8, 10, 12 and 16 h.

84 °C the occurrence of spontaneous solidification dropped as the charge duration increased from 8 to 10 and 12 h.

The large error bars for each the occurrences in Fig. 12 to Fig. 17 shows that the repeatability is rather low and the uncertainty is relatively high.

### 3.4. Tank performances

The total performance of the 10 tanks in 125 test cycles is presented in Fig. 18. Spontaneous solidification occurred 357 times during discharge, 114 times from the cold storage period and 779 times (62 %) the PCM was supercooled for 3 days. In 3 of the 125 test cycles (test cycles 12, 34 and 100) all tanks supercooled stable for 3 days and in one of the test cycles only 2 of the 10 tanks supercooled stable (test series 20, charge at 94 °C for 12 h).

Table 3 shows how often spontaneous solidification occurred during discharge, from the cold storage period and how often the stable supercooling occurred for each of the 10 tanks for all 125 completed test cycles – there was a large deviation of how each individual tank performed even though they were subject to the same test conditions. Tanks T01 and T10 performed the best and achieved stable supercooling in 84 % and 87 % of the test cycles. Tanks T05 performed the worst with only stable supercooling in 30 % of the test cycles.

Table 4 shows how the spontaneous solidification and supercooling stability changed from experiment A to experiment B. On average, there was a higher occurrence of stable supercooling in experiment A compared to B. This was most likely because the discharge temperature was higher in some test cycles in experiment A. Further, it can be seen that tanks T01, T09 and T10 performed relatively similarly in experiment A and B with only a small change in performance. Tanks T02, T03, T06, generally performed worse in experiment B compared to A with more spontaneous solidification both during discharge and from the storage period. Tanks T04, T05 and T08 had similar occurrences of stable supercooling in experiment A and B but the spontaneous solidification shifted from occurring in the in standby period to occurring during the discharge. Tank T07 showed to achieve more stable supercooling in experiment B compared to A.

### 3.5. Solidification starting point

When the crystal blower initiated the solidification, the solidification started from the top of the PCM mantle. The first temperature increase

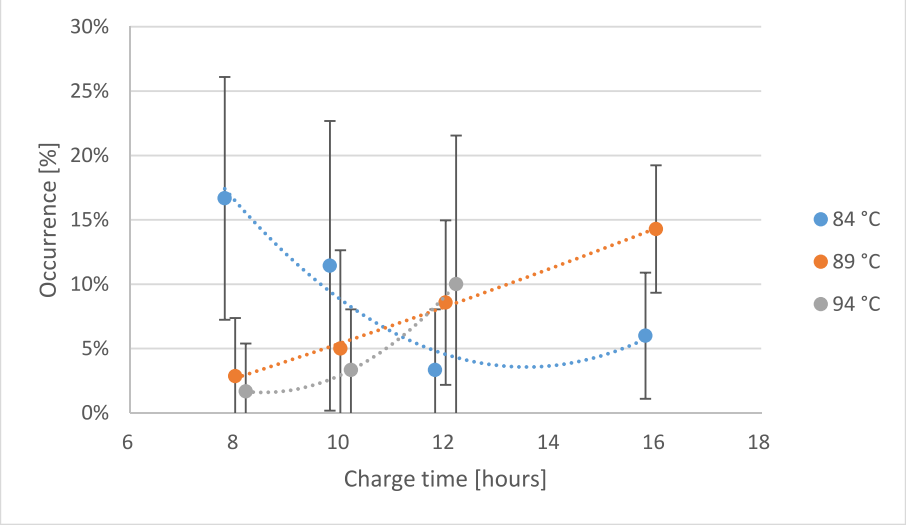


**Fig. 17.** Spontaneous solidification from the supercooled standby period after being charged with 84 °C, 89 °C and 94 °C for 8, 10, 12 and 16 h.

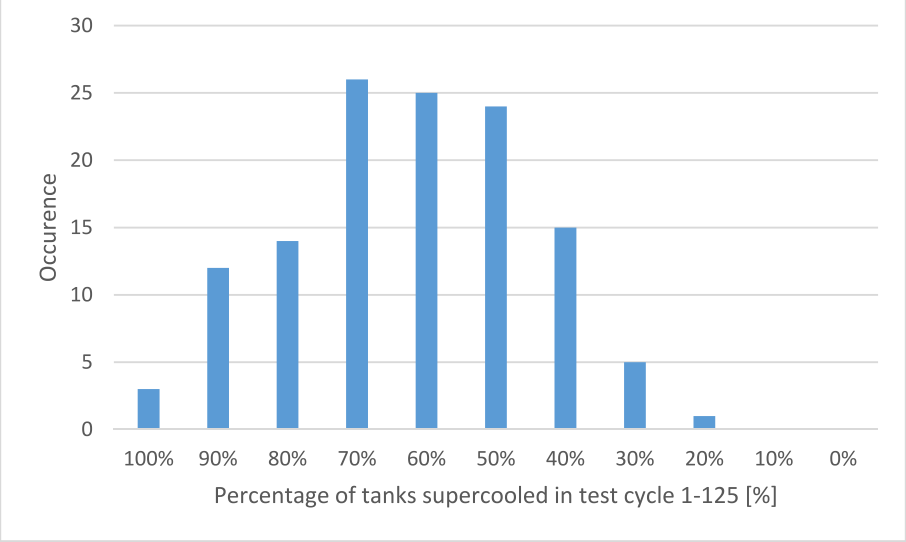


**Fig. 18.** Number of tanks that were table supercooled in 3 days for the 125 test cycles.

**Table 3**
Occurrence of spontaneous solidification during discharge, spontaneous solidification in the cold storage period and stable supercooling for each tank for the 125 test cycles.

| Test series 1-20, Exp. A+B | T01 | T02 | T03 | T04 | T05 | T06 | T07 | T08 | T09 | T10 | all |
|---|---|---|---|---|---|---|---|---|---|---|---|
| Spont. solid. during discharge | 13 % | 43 % | 21 % | 29 % | 44 % | 52 % | 22 % | 18 % | 33 % | 10 % | 29 % |
| Spont. solid. in storage period | 3 % | 2 % | 14 % | 16 % | 26 % | 3 % | 7 % | 10 % | 7 % | 2 % | 9 % |
| Stable supercooling | 84 % | 55 % | 66 % | 55 % | 30 % | 45 % | 70 % | 71 % | 60 % | 87 % | 62 % |

**Table 4**
Changes in spontaneous solidification and supercooling from experiment A to experiment B. (negative values means fewer occurrences in experiment B compared to A, positive values mean more occurrences in experiment B compared to A).

| Change Exp A→Exp B | T01 | T02 | T03 | T04 | T05 | T06 | T07 | T08 | T09 | T10 | all |
|---|---|---|---|---|---|---|---|---|---|---|---|
| Spont. solid. during discharge | 1 % | 10 % | 18 % | 13 % | 25 % | 39 % | −11 % | 14 % | 4 % | −4 % | −11 % |
| Spont. solid. from cold | 6 % | 3 % | 15 % | −16 % | −20 % | 3 % | −3 % | −17 % | −3 % | 1 % | 3 % |
| Stable supercooling | −6 % | −13 % | −33 % | 3 % | −5 % | −42 % | 14 % | 3 % | −1 % | 3 % | −8 % |

was registered at sensor "1U" in all cases.

The longest streak of stable supercooling occurred in tank T07, which supercooled stable 23 times in a row in test cycles 31 to 53. However, this tank also solidified spontaneously 11 times in a row in test cycles 1 to 11. T05 solidified spontaneously 46 times in a row in test cycles 44 to 92 and in test cycles 113 to 117 it was stable supercooled 5 times in a row. In tanks T01 and T10, the occurrences of spontaneous solidification were relatively evenly distributed over all the test cycles without any clear tendency or correlation to the charge and discharge conditions.

Table 5 to Table 8 shows a summary of where the spontaneous solidification occurred for each tank. Table 5 shows an overview of the solidification starting point when solidification occurred during discharge. "NC-SF" represents that it was not clear where the solidification started due to sensor failure or data loss. Only one temperature sensor in the bottom of tank T06 was functioning in part of the test cycles. It was therefore not clear where in the bottom the solidification started in some tests. "XL" represents that the solidification started at the bottom of the PCM mantle.

Overall, it was observed that when solidification occurred during the discharge, the solidification started at the bottom of the PCM mantle in at least 85 % of the cases. The solidification was recorded to start at all of the different lower temperature sensors at some point over all the test cycles. However, it appears that the solidifications occurred more frequently at some sensors in some tanks. E.g., in T05 where the solidification appeared to start near sensor 3 l in 35 of the 55 cases. The 9 times the solidification started near sensor 2M in T06, it was within 11 consecutive test cycles (test cycles 61 to 72). In 6 % of the cases, the PCM appeared to solidify without supercooling (no super.) at around 54 °C and it was not possible to trace where the solicitation started.

As the tanks were discharged with the hot water draw off from the top and the cold water inlet to the bottom of the tank, the discharge process may favor solidification starting from the bottom.

Table 6 shows an analysis of solidification start-temperatures when the solidification occurred during discharge for experiment B, where the tanks were discharged to approximately 10 °C. In 12 % of the cases the solidification occurred without any supercooling registered. Even T01, which generally performed well, had 3 of the 9 cases where the solidification occurred without supercooling. In 8 of the 10 tanks spontaneous solidification occurred at least once without supercooling during discharge.

Table 7 shows an analysis of solidification start-locations when solidification occurred in the cold supercooled standby period. The solidification started from the bottom in 82 % of the cases. In T05 the solidification appeared to start near sensor 3 l in 26 of the 33 cases. In T08 the solidification appeared to start near sensor 2L in 11 of the 13 cases. In T03, the solidification started in the upper part of the PCM mantle in 10 of the 17 cases.

Table 8 shows an analysis of how long the SAT was in the supercooled storage period before spontaneous solidification started. The solidification occurred in all the selected time intervals. There is a slight tendency that the solidification tended to happen earlier rather than later. The tendency indicates that if the storage periods were extended over the 3 days, some spontaneous solidification would be likely to occur at some point in the following time intervals.

### 3.6. Perspective

The spontaneous solidification occurred without a clear pattern. The theory on heterogeneous nucleation indicates that any surface or impurity in the supercooled PCM will pose a risk to form nuclei and start solidification [62]. Rough and unsmooth surfaces are more likely to have structures where nuclei can form. Also, high cooling rates are listed as causes of nucleation. The reason that the spontaneous solidifications in most cases started from the bottom of the tanks may be that impurities in the PCM has settled to the bottom of the mantle or that multiple surfaces were welded together in the bottom of the PCM chambers which could lead to less smooth surfaces. That the spontaneous solidification started at many different locations indicates that there are multiple locations in the PCM chamber where nuclei were formed. If spontaneous solidification starts from impurities or surfaces, it may be difficult, with the current knowledge, to avoid spontaneous solidification completely with the current design. Potentially, another tank material could result in more stable supercooling. It cannot be excluded that there are other reasons for the spontaneous solidification than impurities and the PCM chamber surface such as vibrations or pressure change.

The supercooling stability was higher with higher discharge temperatures – corresponding to low cooling rates of the SAT composite. This may lead to an opportunity to look at systems where the discharge temperature is higher compared to a cold-water inlet, e.g., for space heating. In these investigations the storage tanks were fully discharged in one go. A more realistic domestic hot water draw off pattern may result in a lower cooling rate. A system design that allows for some occasionally spontaneous solidifications may be acceptable if solidified tanks can be reheated and then supercool in the following discharge.

The randomness of the results related to spontaneous solidification shows that more research is needed to fully understand the behavior of supercooled SAT in building application.

**Table 5**
Overview of solidification starting point when solidification occurred during discharge.

| Tank<br>Sensor | T01 | T02 | T03 | T04 | T05 | T06 | T07 | T08 | T09 | T10 | All | % |
|---|---|---|---|---|---|---|---|---|---|---|---|---|
| 1U | 0 | 0 | 0 | 0 | 0 | 0 | 0 | 0 | 1 | 0 | 1 | 0 % |
| 2U | 0 | 0 | 1 | 0 | 0 | 0 | 0 | 0 | 0 | 0 | 1 | 0 % |
| 3U | 0 | 0 | 1 | 0 | 0 | 0 | 0 | 1 | 0 | 0 | 2 | 1 % |
| 4U | 0 | 0 | 0 | 2 | 0 | 0 | 0 | 0 | 1 | 0 | 3 | 1 % |
| 1M | 0 | 0 | 1 | 1 | 0 | 0 | 0 | 0 | 0 | 0 | 2 | 1 % |
| 2M | 0 | 0 | 1 | 1 | 0 | 9 | 0 | 0 | 0 | 0 | 11 | 3 % |
| 3M | 0 | 0 | 0 | 0 | 0 | 0 | 0 | 0 | 0 | 0 | 0 | 0 % |
| 4M | 0 | 0 | 1 | 0 | 0 | 0 | 0 | 0 | 0 | 0 | 1 | 0 % |
| 1L | 5 | 3 | 5 | 5 | 8 | 9 | 4 | 4 | 17 | 7 | 67 | 19 % |
| 2L | 1 | 18 | 4 | 9 | 5 | 10 | 5 | 7 | 8 | 1 | 68 | 19 % |
| 3L | 2 | 15 | 5 | 8 | 35 | 8 | 2 | 5 | 8 | 1 | 89 | 25 % |
| 4L | 5 | 3 | 7 | 9 | 6 | 5 | 15 | 2 | 4 | 4 | 60 | 17 % |
| XL | | | | | | 18 | | | | | 18 | 5 % |
| NC-SF | 0 | 10 | 0 | 0 | 0 | 4 | 0 | 0 | 0 | 0 | 14 | 4 % |
| Nosuper. | 3 | 5 | 0 | 1 | 1 | 2 | 2 | 4 | 2 | 0 | 20 | 6 % |
| Total | 16 | 54 | 26 | 36 | 55 | 65 | 28 | 23 | 41 | 13 | 357 | 100 % |

**Table 6**
Overview of solidification temperature when solidification occurred during discharge in experiment B.

| Tank<br>Temp. | T01 | T02 | T03 | T04 | T05 | T06 | T07 | T08 | T09 | T10 | All | % |
|---|---|---|---|---|---|---|---|---|---|---|---|---|
| <20 °C | 2 | 5 | 7 | 9 | 5 | 5 | 6 | 3 | 9 | 1 | 52 | 23 % |
| 20-53 °C | 4 | 16 | 13 | 14 | 29 | 39 | 3 | 11 | 9 | 5 | 143 | 62 % |
| 53-58 °C | 3 | 4 | 0 | 1 | 4 | 0 | 3 | 3 | 6 | 0 | 24 | 10 % |
| NC-SF | 0 | 8 | 0 | 0 | 0 | 4 | 0 | 0 | 0 | 0 | 12 | 5 % |
| Total | 9 | 33 | 20 | 24 | 38 | 48 | 12 | 17 | 24 | 6 | 231 | 100 % |

**Table 7**
Overview of solidification starting point when the solidification started in the cold supercooled standby period.

| Tank<br>Sensor | T01 | T02 | T03 | T04 | T05 | T06 | T07 | T08 | T09 | T10 | All | % |
|---|---|---|---|---|---|---|---|---|---|---|---|---|
| 1U | 1 | 0 | 5 | 1 | 0 | 0 | 0 | 0 | 1 | 2 | 10 | 9 % |
| 2U | 0 | 0 | 2 | 0 | 0 | 0 | 0 | 0 | 0 | 0 | 2 | 2 % |
| 3U | 0 | 0 | 0 | 0 | 0 | 0 | 0 | 0 | 0 | 0 | 0 | 0 % |
| 4U | 0 | 0 | 3 | 0 | 0 | 0 | 0 | 0 | 0 | 0 | 3 | 3 % |
| 1M | 0 | 0 | 0 | 0 | 0 | 1 | 0 | 0 | 0 | 0 | 1 | 1 % |
| 2M | 0 | 0 | 1 | 0 | 0 | 0 | 0 | 0 | 0 | 0 | 1 | 1 % |
| 3M | 0 | 0 | 0 | 0 | 0 | 0 | 0 | 0 | 1 | 0 | 1 | 1 % |
| 4M | 0 | 0 | 2 | 0 | 0 | 0 | 0 | 0 | 1 | 0 | 3 | 3 % |
| 1L | 2 | 0 | 2 | 12 | 4 | 2 | 2 | 1 | 2 | 0 | 27 | 24 % |
| 2L | 0 | 0 | 1 | 0 | 3 | 1 | 2 | 11 | 0 | 0 | 18 | 16 % |
| 3L | 0 | 2 | 0 | 3 | 26 | 0 | 1 | 1 | 0 | 0 | 33 | 29 % |
| 4L | 1 | 0 | 1 | 4 | 0 | 0 | 4 | 0 | 4 | 1 | 15 | 13 % |
| Total | 4 | 2 | 17 | 20 | 33 | 4 | 9 | 13 | 9 | 3 | 114 | 100 % |

**Table 8**
Overview of supercooled storage period before spontaneous solidification from cold.

| Tank<br>Time | T01 | T02 | T03 | T04 | T05 | T06 | T07 | T08 | T09 | T10 | All | % |
|---|---|---|---|---|---|---|---|---|---|---|---|---|
| 0–10 h | 2 | 0 | 3 | 5 | 8 | 0 | 4 | 1 | 2 | 0 | 25 | 22 % |
| 10–20 h | 0 | 1 | 3 | 3 | 5 | 1 | 1 | 2 | 0 | 0 | 16 | 14 % |
| 20–30 h | 1 | 0 | 4 | 5 | 3 | 1 | 1 | 1 | 1 | 0 | 17 | 15 % |
| 30–40 h | 1 | 0 | 0 | 3 | 5 | 1 | 0 | 2 | 3 | 0 | 15 | 13 % |
| 40–50 h | 0 | 0 | 2 | 0 | 3 | 0 | 0 | 4 | 2 | 0 | 11 | 10 % |
| 50–60 h | 0 | 0 | 3 | 2 | 6 | 0 | 1 | 3 | 0 | 3 | 18 | 16 % |
| 60–72 h | 0 | 1 | 2 | 2 | 3 | 1 | 2 | 0 | 1 | 0 | 12 | 11 % |
| Total | 4 | 2 | 17 | 20 | 33 | 4 | 9 | 13 | 9 | 3 | 114 | 100 % |

## 4. Conclusions

This research showed that stable supercooling was achieved in up to 87 % of the test cycles in heat storage units utilizing 35 kg of SAT composite in tanks built in stainless steel. However, the behavior of the supercooling was somewhat unpredictable. Temperature and durations had some effect on the supercooling stability. The construction of the individual tank or impurities in the PCM most likely influenced the ability of the SAT to remain supercooled in the PCM chambers on some tanks in particular. Careful manufacturing or other tank materials may allow for more stable performance if the surfaces in contact with the PCM are more smooth and cracks and impurities are avoided.

The supercooling stability in 10 identical heat storage units utilizing stable supercooling of a sodium acetate trihydrate composite has been tested. A systematic test strategy was applied to determine the influence of charge- and discharge conditions. Each of the tested conditions was repeated 5–7 times. There was a large spread in the results. Thus, a large number of test series was applied – their analysis resulted in the following findings:

- Across all test cycles, supercooling for 3 days was achieved in 62 % of the cases. However, stable supercooling was achieved in up to 85 % of the test cycles when the discharge temperature was 25–35 °C. The occurrence of supercooling was lower with lower discharge temperatures.
- Across all test cycles, the spontaneous solidification occurred during the discharge in 29 % of the cases and 9 % of the cases during the 3 days cold standby period. The starting location of the crystallization during discharge and in the period of supercooling (standby) was at the bottom part of the PCM mantle in 85 % and 82 % of the cases.
- The performance of individual tanks deviated a lot. The best performing tank supercooled stable for the 3 days in 87 % of the test cycles and the worst performing tank supercooled stable in 30 % of the test cycles.
- Both charging and discharging temperatures showed significant influence on the supercooling stability during discharge. The occurrence of spontaneous solidification from cold, supercooled state (standby) depended largely on charging conditions, while the discharge temperature had relatively little influence.
- The charge duration that resulted in the highest occurrence of stable supercooling was 12 h with 84 °C, 10 h with 89 °C and 8 h with 94 °C. Longer charge durations resulted in lower occurrence of stable supercooling.

### CRediT authorship contribution statement

**Mark Dannemand:** Conceptualization, Data curation, Formal analysis, Funding acquisition, Investigation, Methodology, Project administration, Writing – original draft, Writing – review & editing, Supervision, Visualization. **Gerald Englmair:** Data curation, Formal

analysis, Investigation, Methodology, Writing – original draft, Writing – review & editing. **Weiqiang Kong:** Data curation, Investigation, Writing – review & editing. **Simon Furbo:** Conceptualization, Formal analysis, Funding acquisition, Investigation, Methodology, Supervision, Writing – review & editing.

## Declaration of competing interest

The authors declare the following financial interests/personal relationships which may be considered as potential competing interests: Mark Dannemand reports financial support and equipment, drugs, or supplies were provided by H.M. Heizkörper GmbH Heating Technology.

## Data availability

Data will be made available on request.

## Acknowledgements

H.M. Heizkörper GmbH & Co KG manufactured the storage tanks and financed the research. We thank the DTU research technicians Lars Kokholm Andersen and Claus Aagaard for their practical support.

## References

[1] EuropeanParliament, EU Energy Efficiency Directive 2012/27/EU of the European Parliament and of the council of 25 October 2012, amending Directives 2009/125/EC and 2010/30/EU and repealing Directives 2004/8/EC and 2006/32/EC, Off. J. Eur. Union L 315/3 (2012).
[2] S. Colclough, T. McGrath, Net energy analysis of a solar combi system with seasonal thermal energy store, Appl. Energy 147 (2015) 611–616, https://doi.org/10.1016/j.apenergy.2015.02.088.
[3] D. Heide, L. von Bremen, M. Greiner, C. Hoffmann, M. Speckmann, S. Bofinger, Seasonal optimal mix of wind and solar power in a future, highly renewable Europe, Renew. Energy 35 (2010) 2483–2489, https://doi.org/10.1016/j.renene.2010.03.012.
[4] L.F. Cabeza, L. Miró, E. Oró, A. de Gracia, V. Martin, A. Kroenauer, et al., CO2 mitigation accounting for Thermal Energy Storage (TES) case studies, Appl. Energy 155 (2015) 365–377, https://doi.org/10.1016/j.apenergy.2015.05.121.
[5] W. Weiss (Ed.), Solar Heating Systems for Houses, a Design Handbook for Solar Combisystems, James & James Ltd., UK, 2003.
[6] C. Finck, R. Li, R. Kramer, W. Zeiler, Quantifying demand fl exibility of power-to-heat and thermal energy storage in the control of building heating systems, Appl. Energy 209 (2018) 409–425, https://doi.org/10.1016/j.apenergy.2017.11.036.
[7] W. Kramer, A. Oliva, G. Stryi-Hipp, S. Kobelt, D. Bestenlehner, H. Drück, et al., Solar-active-houses - analysis of the building concept based on detailed measurements, Energy Procedia 48 (2014) 895–903, https://doi.org/10.1016/j.egypro.2014.02.103.
[8] A. Oliva, G. Stryi-Hipp, S. Kobelt, D. Bestenlehner, H. Drück, G. Dasch, Solar-active-houses - dynamic system simulations to analyze building concepts with high fractions of solar thermal energy, Energy Procedia 70 (2015) 652–660, https://doi.org/10.1016/j.egypro.2015.02.173.
[9] A. Ristić, S. Furbo, C. Moser, H. Schranzhofer, A. Lazaro, M. Delgado, et al., IEA SHC Task 42 / ECES Annex 29 WG A1: Engineering and Processing of PCMs, TCMs and Sorption Materials. Energy Procedia 91, 2016, pp. 207–217, https://doi.org/10.1016/j.egypro.2016.06.205.
[10] B. Zettl, G. Englmair, W. Somitsch, An open sorption heat storage concept and materials for building heat supply, Energy Procedia 73 (2015) 297–304, https://doi.org/10.1016/j.egypro.2015.07.692.
[11] B. Zettl, H. Kirchsteiger, An open sorption heat storage application, in: Int. Sustain. Energy Conf. 2018, Graz, Austria: AEE Intec, 2018, pp. 605–611.
[12] T. Nonnen, S. Beckert, K. Gleichmann, A. Brandt, B. Unger, H. Kerskes, et al., A thermochemical long-term heat storage system based on a salt/zeolite composite, Chem. Eng. Technol. 39 (2016) 2427–2434, https://doi.org/10.1002/ceat.201600301.
[13] R. Köll, W. van Helden, G. Engel, W. Wagner, B. Dang, J. Jänchen, et al., An experimental investigation of a realistic-scale seasonal solar adsorption storage system for buildings, Sol. Energy 155 (2017) 388–397, https://doi.org/10.1016/j.solener.2017.06.043.
[14] B. Fumey, R. Weber, L. Baldini, Liquid sorption heat storage – a proof of concept based on lab measurements with a novel spiral fined heat and mass exchanger design, Appl. Energy 200 (2017) 215–225, https://doi.org/10.1016/j.apenergy.2017.05.056.
[15] M. Dannemand, J.M. Schultz, J.B. Johansen, S. Furbo, Long term thermal energy storage with stable supercooled sodium acetate trihydrate, Appl. Therm. Eng. 91 (2015) 671–678, https://doi.org/10.1016/j.applthermaleng.2015.08.055.
[16] B. Zalba, J.M. Marín, L.F. Cabeza, H. Mehling, Review on thermal energy storage with phase change: materials, heat transfer analysis and applications, Appl. Therm. Eng. 23 (2003) 251–283.
[17] H. Mehling, L.F. Cabeza, Heat and Cold Stroage with PCM. Vo. 308, Springer, Berlin, 2008.
[18] N. Beaupere, U. Soupremanien, L. Zalewski, Nucleation triggering methods in supercooled phase change materials (PCM), a review, Thermochim. Acta 670 (2018) 184–201, https://doi.org/10.1016/j.tca.2018.10.009.
[19] P.F. Barrett, B.R. Best, Thermal energy storage in supercooled salt mixtures, Mater. Chem. Phys. 12 (1985) 529–536.
[20] B. Sandnes, J. Rekstad, Supercooling salt hydrates: stored enthalpy as a function of temperature, Sol. Energy 80 (2006) 616–625, https://doi.org/10.1016/j.solener.2004.11.014.
[21] S.M. Hasnain, Review on sustainable thermal energy storage technologies, part II: cool thermal storage, Energy Convers. Manag. 39 (1998) 1139–1153, https://doi.org/10.1016/S0196-8904(98)00024-7.
[22] H.P. Garg, M. Nasim, Studies on low-temperature salt-hydrate for thermal storage applications, Energy Convers. Manag. 21 (1981) 125–130, https://doi.org/10.1016/0196-8904(81)90033-9.
[23] T. Xu, S.N. Gunasekara, J.N. Chiu, B. Palm, S. Sawalha, Thermal behavior of a sodium acetate trihydrate-based PCM: T-history and full-scale tests, Appl. Energy (2020) 261, https://doi.org/10.1016/j.apenergy.2019.114432.
[24] N. Beaupere, U. Soupremanien, L. Zalewski, Experimental measurements of the residual solidification duration of a supercooled sodium acetate trihydrate, Int. J. Therm. Sci. (2020) 158, https://doi.org/10.1016/j.ijthermalsci.2020.106544.
[25] S.N. Gunasekara, R. Pan, J.N. Chiu, V. Martin, Polyols as phase change materials for surplus thermal energy storage q, Appl. Energy 162 (2016) 1439–1452, https://doi.org/10.1016/j.apenergy.2015.03.064.
[26] A. Seppälä, A. Meriläinen, L. Wikström, P. Kauranen, The effect of additives on the speed of the crystallization front of xylitol with various degrees of supercooling, Exp. Thermal Fluid Sci. 34 (2010) 523–527, https://doi.org/10.1016/j.expthermflusci.2009.11.005.
[27] M. Duquesne, E.P. Del Barrio, A. Godin, Nucleation triggering of highly undercooled Xylitol using an air lift reactor for seasonal thermal energy storage, Appl. Sci. (2019) 9, https://doi.org/10.3390/app9020267.
[28] S. Puupponen, A. Seppälä, Cold-crystallization of polyelectrolyte absorbed polyol for long-term thermal energy storage, Sol. Energy Mater. Sol. Cells 180 (2018) 59–66, https://doi.org/10.1016/j.solmat.2018.02.013.
[29] M.A. Rogerson, S.S.S. Cardoso, Solidification in heat packs: I. Nucleation rate, AICHE J. 49 (2003) 505–515, https://doi.org/10.1002/aic.690490220.
[30] W. Kong, M. Dannemand, J. Berg Johansen, J. Fan, S. Furbo, Experimental investigations on phase separation for different heights of sodium acetate water mixtures under different conditions, Appl. Therm. Eng. 148 (2018) 796–805, https://doi.org/10.1016/j.applthermaleng.2018.10.017.
[31] M. Dannemand, J.B. Johansen, S. Furbo, Solidification behavior and thermal conductivity of bulk sodium acetate trihydrate composites with thickening agents and graphite, Sol. Energy Mater. Sol. Cells 145 (2016) 287–295, https://doi.org/10.1016/j.solmat.2015.10.038.
[32] G. Englmair, S. Furbo, M. Dannemand, J. Fan, Experimental investigation of a tank-in-tank heat storage unit utilizing stable supercooling of sodium acetate trihydrate, Appl. Therm. Eng. 167 (2020) 114709, https://doi.org/10.1016/j.applthermaleng.2019.114709.
[33] Z. Khan, Z. Khan, A. Ghafoor, A review of performance enhancement of PCM based latent heat storage system within the context of materials, thermal stability and compatibility, Energy Convers. Manag. 115 (2016) 132–158, https://doi.org/10.1016/j.enconman.2016.02.045.
[34] Y. Wang, K. Yu, X. Ling, Experimental and modeling study on thermal performance of hydrated salt latent heat thermal energy storage system, Energy Convers. Manag. 198 (2019) 111796, https://doi.org/10.1016/j.enconman.2019.111796.
[35] W. Cui, Y. Yuan, L. Sun, X. Cao, X. Yang, Experimental studies on the supercooling and melting/freezing characteristics of nano-copper/sodium acetate trihydrate composite phase change materials, Renew. Energy 99 (2016) 1029–1037, https://doi.org/10.1016/j.renene.2016.08.001.
[36] J. Guion, M. Teisseire, Nucleation of sodium acetate trihydrate in thermal heat storage cycles, Sol. Energy 46 (1991) 97–100.
[37] M. Dannemand, J. Dragsted, J. Fan, J.B. Johansen, W. Kong, S. Furbo, Experimental investigations on prototype heat storage units utilizing stable supercooling of sodium acetate trihydrate mixtures, Appl. Energy 169 (2016) 72–80, https://doi.org/10.1016/j.apenergy.2016.02.038.
[38] M. Dannemand, J.B. Johansen, W. Kong, S. Furbo, Experimental investigations on cylindrical latent heat storage units with sodium acetate trihydrate composites utilizing supercooling, Appl. Energy 177 (2016) 591–601, https://doi.org/10.1016/j.apenergy.2016.05.144.
[39] G. Englmair, C. Moser, S. Furbo, M. Dannemand, J. Fan, Design and functionality of a segmented heat-storage prototype utilizing stable supercooling of sodium acetate trihydrate in a solar heating system, Appl. Energy 221 (2018) 522–534, https://doi.org/10.1016/j.apenergy.2018.03.124.
[40] G. Wang, M. Dannemand, C. Xu, G. Englmair, S. Furbo, J. Fan, Thermal characteristics of a long-term heat storage unit with sodium acetate trihydrate, Appl. Therm. Eng. (2021) 187, https://doi.org/10.1016/j.applthermaleng.2021.116563.
[41] G. Englmair, W. Kong, J.B. Berg, S. Furbo, J. Fan, Demonstration of a solar combi-system utilizing stable supercooling of sodium acetate trihydrate for heat storage, Appl. Therm. Eng. 166 (2020) 114647, https://doi.org/10.1016/j.applthermaleng.2019.114647.

[42] G. Englmair, C. Moser, H. Schranzhofer, J. Fan, S. Furbo, A solar combi-system utilizing stable supercooling of sodium acetate trihydrate for heat storage: numerical performance investigation, Appl. Energy 242 (2019) 1108–1120, https://doi.org/10.1016/j.apenergy.2019.03.125.
[43] L. Dietz, J.S. Brukner, C.A. Hollingsworth, Linear crystallization velocities of sodium acetate in supersaturated solutions, J. Phys. Chem. 61 (1957) 944–948, https://doi.org/10.1021/j150553a023.
[44] G. Englmair, Y. Jiang, M. Dannemand, C. Moser, H. Schranzhofer, S. Furbo, et al., Crystallization by local cooling of supercooled sodium acetate trihydrate composites for long-term heat storage, Energ. Build. 180 (2018) 159–171, https://doi.org/10.1016/j.enbuild.2018.09.035.
[45] J.W. Mullin, Crystallization, Butterworth-Heinemann, Fourth Edi. Oxford, 2001.
[46] N. Araki, M. Futamura, A. Makino, H. Shibata, Measurements of thermophysical properties of sodium acetate hydrate, Int. J. Thermophys. 16 (1995) 1455–1466.
[47] M.A. Rogerson, S.S.S. Cardoso, Solidification in heat packs: III. Metallic trigger, AICHE J. 49 (2003) 522–529, https://doi.org/10.1002/aic.690490222.
[48] A. Awasthi, N.A. Shah, Y. Jeon, O.K. Kwon, J.D. Chung, Super-cooling effects and solidification of water inside a horizontal cylinder with a rough, sinusoidal surface shape, J. Energy Storage (2022) 51, https://doi.org/10.1016/j.est.2022.104442.
[49] G. Wang, C. Xu, W. Kong, G. Englmair, J. Fan, G. Wei, et al., Review on sodium acetate trihydrate in flexible thermal energy storages: properties, challenges and applications, J. Energy Storage (2021) 40, https://doi.org/10.1016/j.est.2021.102780.
[50] G. Wang, Z. Liao, C. Xu, G. Englmair, W. Kong, J. Fan, et al., Design optimization of a latent heat storage using sodium acetate trihydrate, J. Energy Storage (2022) 52, https://doi.org/10.1016/j.est.2022.104798.
[51] I. Shamseddine, F. Pennec, P. Biwole, F. Fardoun, Supercooling of phase change materials: a review, Renew. Sust. Energ. Rev. 158 (2022), https://doi.org/10.1016/j.rser.2022.112172.
[52] C. Kutlu, E. Tapia-Brito, O. Agbonaye, Y. Su, S.T. Smith, B. Hughes, et al., Incorporation of controllable supercooled phase change material heat storage with a solar assisted heat pump: testing of crystallization triggering and heating demand-based modelling study, J. Energy Storage 55 (2022), https://doi.org/10.1016/j.est.2022.105744.
[53] H. Wang, Y. Hu, F. Jiang, X. Ling, Thermal performance of industrial-grade CH3COONa·3H2O-based composite phase change materials in a plate heat storage unit, Energy (2022) 261, https://doi.org/10.1016/j.energy.2022.125232.
[54] S. Chen, C. Yu, G. Wang, W. Kong, Z. Tian, J. Fan, Heat transfer of a shell and tube sodium acetate trihydrate heat storage tank, J. Energy Storage (2022) 55, https://doi.org/10.1016/j.est.2022.105600.
[55] G. Zhou, Y. Li, M. Zhu, Experimental investigation on space heating performances of supercooled thermal storage units with sodium acetate trihydrate, Energ. Build. (2022) 271, https://doi.org/10.1016/j.enbuild.2022.112329.
[56] G. Ferrer, A. Solé, C. Barreneche, I. Martorell, L.F. Cabeza, Review on the methodology used in thermal stability characterization of phase change materials, Renew. Sust. Energ. Rev. 50 (2015) 665–685, https://doi.org/10.1016/j.rser.2015.04.187.
[57] C. Rathgeber, A. Grisval, H. Schmit, P. Hoock, S. Hiebler, Concentration dependent melting enthalpy, crystallization velocity, and thermal cycling stability of pinacone hexahydrate, Thermochim. Acta 670 (2018) 142–147, https://doi.org/10.1016/j.tca.2018.10.025.
[58] W. Kong, M. Dannemand, J.B. Johansen, J. Fan, J. Dragsted, G. Englmair, et al., Experimental investigations on heat content of supercooled sodium acetate trihydrate by a simple heat loss method, Sol. Energy 139 (2016) 249–257, https://doi.org/10.1016/j.solener.2016.09.045.
[59] C. Rathgeber, S. Hiebler, R. Bayón, L.F. Cabeza, G. Zsembinszki, G. Englmair, et al., Experimental devices to investigate the long-term stability of phase change materials under application conditions, Appl. Sci. (Switzerland) 10 (2020) 1–30, https://doi.org/10.3390/app10227968.
[60] R. Bayón, E. Rojas, Development of a new methodology for validating thermal storage media: application to phase change materials, Int. J. Energy Res. 43 (2019) 6521–6541, https://doi.org/10.1002/er.4589.
[61] J. Deng, S. Furbo, W. Kong, J. Fan, Thermal performance assessment and improvement of a solar domestic hot water tank with PCM in the mantle, Energ. Build. 172 (2018) 10–21, https://doi.org/10.1016/j.enbuild.2018.04.058.
[62] G. Wypych, Handbook of Nucleating Agents, Elsevier, 2016, https://doi.org/10.1016/C2015-0-01461-7.